International Journal of Applied Earth Observation and Geoinformation 43 (2015) 55–83

Contents lists available at ScienceDirect

International Journal of Applied Earth Observation and Geoinformation

journal homepage: www.elsevier.com/locate/jag

# Plant phenolics and absorption features in vegetation reflectance spectra near 1.66 μm

Raymond F. Kokaly[a,*], Andrew K. Skidmore[b]

[a] U.S Geological Survey (USGS), MS 973 Box 25046, Denver Federal Center, Denver, Colorado 80225, USA
[b] Faculty of Geo-Information Science and Earth Observation (ITC), University of Twente, P.O. Box 217, 7500 AE Enschede, The Netherlands

ARTICLE INFO

*Article history:*
Available online 7 February 2015

*Keywords:*
Canopy chemistry
Spectroscopy
Remote sensing
Continuum removal
Spectral feature analysis
Tannin
Polyphenols

ABSTRACT

Past laboratory and field studies have quantified phenolic substances in vegetative matter from reflectance measurements for understanding plant response to herbivores and insect predation. Past remote sensing studies on phenolics have evaluated crop quality and vegetation patterns caused by bedrock geology and associated variations in soil geochemistry. We examined spectra of pure phenolic compounds, common plant biochemical constituents, dry leaves, fresh leaves, and plant canopies for direct evidence of absorption features attributable to plant phenolics. Using spectral feature analysis with continuum removal, we observed that a narrow feature at 1.66 μm is persistent in spectra of manzanita, sumac, red maple, sugar maple, tea, and other species. This feature was consistent with absorption caused by aromatic C—H bonds in the chemical structure of phenolic compounds and non-hydroxylated aromatics. Because of overlapping absorption by water, the feature was weaker in fresh leaf and canopy spectra compared to dry leaf measurements. Simple linear regressions of feature depth and feature area with polyphenol concentration in tea resulted in high correlations and low errors (% phenol by dry weight) at the dry leaf ($r^2$ = 0.95, RMSE = 1.0%, $n$ = 56), fresh leaf ($r^2$ = 0.79, RMSE = 2.1%, $n$ = 56), and canopy ($r^2$ = 0.78, RMSE = 1.0%, $n$ = 13) levels of measurement. Spectra of leaves, needles, and canopies of big sagebrush and evergreens exhibited a weak absorption feature centered near 1.63 μm, short ward of the phenolic compounds, possibly consistent with terpenes. This study demonstrates that subtle variation in vegetation spectra in the shortwave infrared can directly indicate biochemical constituents and be used to quantify them. Phenolics are of lesser abundance compared to the major plant constituents but, nonetheless, have important plant functions and ecological significance. Additional research is needed to advance our understanding of the spectral influences of plant phenolics and terpenes relative to dominant leaf biochemistry (water, chlorophyll, protein/nitrogen, cellulose, and lignin).



## Introduction and Background

Variation in plant biochemical composition is a consequence of speciation and adaptation by vegetation to external impacts including climatic and edaphic gradients, predation by insects and animals, plant pathogens, and other influences. The major components of vegetation are fundamental biochemical constituents that are central to their physiological form and function, including water, chlorophyll and accessory pigments, cellulose, starch, sugars, lignin, and protein. These components are commonly the primary focus of laboratory, field and remote sensing studies that seek to use reflectance spectroscopy to estimate biochemical content or concentrations in leaves and plant canopies (Kokaly et al., 2009; Ustin et al., 2009) as well as being the basis of physical radiative transfer models such as PROSPECT (Jacquemoud and Baret, 1990; Jacquemoud et al., 2009).

Nitrogen (N) is highly correlated with protein and it is typically the quantity studied, although nitrogen is in much lower concentration in plants than protein (Kokaly and Clark, 1999; Kokaly, 2001). Other plant constituents with low abundance are receiving increasing attention. Among these are monophenolic and polyphenolic constituents, herein referred to collectively as plant phenolics, which are generally viewed as important for plant defense (Vermerris and Nicholson, 2006). For example, Soukupová et al. (2001), Campbell et al. (2004) attributed increases in plant phenolics in conifer needles as a response to damage caused by air pollution. On a human level, phenolic compounds have been

* Corresponding author. Tel.: +13032361359; fax.: +13032363200.
*E-mail addresses:* raymond@usgs.gov (R.F. Kokaly), a.k.skidmore@utwente.nl (A.K. Skidmore).

http://dx.doi.org/10.1016/j.jag.2015.01.010

the subject of much study for their potential health benefits as antioxidants (Rice-Evans et al., 1996). At the ecosystem level, a recent publication examining the biochemical and species diversity of tropical forests have found plant phenolics to be important for separating taxonomic classes (Asner et al., 2012), though the variation in phenolic concentration within a species as well as between species remains an active area of research (Bian et al., 2013).

In comparison to biochemical constituents with well-defined chemical structures, such as water, chlorophyll, and cellulose, plant phenolics are highly varied in their composition. They only share the occurrence of a phenolic ring structure, a cyclic, six-carbon benzene ring modified to have at least one hydroxyl (—OH) attached to the carbon atoms in the ring. Common plant phenolics with a single ring include phenolic acids (e.g., salicylic acid), hydroxycinnamic acids (e.g., caffeic acid), and coumarins. Polyphenolics, of which there are thousands, include anthocyanidins (e.g., cyanidin), flavonols (e.g., quercetin), and flavanols (e.g., catechin). Many functions are attributed to plant phenolics, including roles as protective pigments and damage inhibitors as pre-formed *phytoanticipins* (van Etten et al., 1994). Plant phenolics can also accumulate in cells in response to pathogens; these constituents are termed *phytoalexins* (e.g., Aguero et al., 2002).

Larger polyphenolics, the tannins, have molecular weights ranging from ~500 to 3000 (Bate-Smith and Swain, 1962). These were initially described as vegetable extracts capable of tanning animal skins (Seguin, 1796). Tannins can cross-link with proteins and inhibit enzymatic activity (Zucker, 1983) and are astringent, giving a dry, puckery feel to the mouth as in cocoa, tea and wines (Swain, 1965). Tannins have been studied for their protective actions against herbivory (Salminen and Karonen, 2011; and the review by Barbehenn and Constabel, 2011). Condensed tannins, also known as proanthocyanidins, are typically oligomers and polymers of catechin, epicatechin and derivatives of these two molecules with mono- or tri-hydroxylated benzene rings (Barbehenn and Constabel, 2011). Hydrolysable tannins are more complex structurally. They are generally divided into three groups: gallic acid derivatives, gallotannins, and ellagitannins (Salminen and Karonen, 2011). Gallic acid derivatives and gallotannins are typified by galloyl groups esterified to glucose or quinic acid (Mueller-Harvey, 2001). More than 500 ellagitannin structures have been described and they occur more frequently in nature than gallotannins (Salminen and Karonen, 2011).

Lignins are a special class of large polyphenol with molecular weight that can be more than 10,000 (Crawford, 1981); however, that value varies dependent on the plant tissue examined and the extraction method (Tolbert et al., 2014). Lignin adds rigidity to plant cell walls and has been recognized for some time as a basic constituent of wood (de Candolle, 1813). Lignin has a poorly-defined structure comprised of phenolic monolignols, primarily, *p*-coumaryl, coniferyl and sinapyl alcohols (Hatfield and Vermerris, 2001).

Because of their chemical variation, it is expected that the spectra of plant phenolics should also vary, with absorption features changing shape and wavelength position based on the substituent groups bound to the phenolic ring. For robust estimation of plant phenolics as a group using reflectance spectra, a persistent and fairly consistent absorption feature is desired that is relatively insensitive to variations in molecules attached to the phenolic ring(s).

Early studies in feed and crop analysis using statistical methods in near-infrared reflectance spectroscopy (NIRS; Norris et al., 1976) indicated that such a consistency might exist for phenolic substances. Windham et al. (1988) predicted the content of tannin with a coefficient of determination of 0.91 in *Lespedeza cuneata* (Dum. -Cours.) G. Don. They noted that reflectance at 1.66 μm was the most important wavelength in the prediction equation. In a review of wavelengths related to foliar chemistry, Curran (1989) listed 1.12, 1.20, 1.42, 1.45, 1.69 μm as wavelengths associated with C—H bonds that might be related to lignin. Elvidge (1990) presented spectra of dried plant components and biochemical constituents, including tannic acid with absorption features centered near 1.46, 1.66, 1.93, 2.13, 2.26, and 2.32 μm, and two forms of lignin with absorption features centered near 1.45, 1.68, 1.93, 2.27, 2.33, and 2.38 μm. Flinn et al. (1996) used NIRS to estimate concentrations of phenolic constituents in the fodder shrub tagasaste (*Chamaecytisus proliferus*), in particular the phenolics luteolin and apigenin. Increased concentrations of the phenolics were found in fodder rejected by sheep. They reported spectral changes in the 1.67 μm region for samples with high phenolic concentration (>20%) compared to samples with low concentration (<2%). Martin and Aber (1997) found that imaging spectrometer data could be related to lignin concentrations in forest canopies using reflectance at four wavelengths, including 1.66 μm. Ben-Dor et al. (1997), in an analysis of reflectance spectra of decomposing organic matter, reported the assignment of 1.669 μm to an overtone of the aromatic C—H bond. Foley et al. (1998) indicated wavelengths near 1.65 μm are expected to be related to phenolic compound content but noted that lignin has absorption near this wavelength.

These early studies indicated the potential for successfully estimating plant phenolic concentrations from wavelength regions. Recently, contributions to the literature on reflectance and plant biochemistry have again turned to plant phenolics. In Ferwerda et al. (2006), a reflectance spectrum of powdered quebracho tannin showed absorption features in the wavelength range of 1.64–1.70 μm. Meggio et al. (2010) used a spectral index analysis of reflectance spectra to estimate anthocyanin and tannin concentrations in grape leaves. Asner et al. (2011) examined a large data set of leaves from humid tropical forest canopies. Although typically less abundant, they reported phenolics reaching 30% and tannins up to 20% concentration. Examining leaf reflectance spectra with partial least squares regression (PLSR), they estimated concentrations of phenols and tannins ($r^2$ = 0.74, and 0.62, respectively). Bian et al. (2010) also used PLSR to relate reflectance to catechin content in tea (*Camellia sinensis*), where the concentration of that polyphenol was found to range from 14 to 29% on a dry leaf basis. With similar methods, Bian et al. (2013) related polyphenol content to reflectance spectra of powdered leaves, whole leaves, and plant canopies, achieving good results with $r^2$ values of 0.91 for powdered leaves, 0.80 for intact leaves, and 0.84 at the canopy level.

Considering the important roles of phenolics in plants, their potential for inhibiting or indicating damage or stress to vegetation, and the wide range of phenolic concentrations in different species, improved knowledge is desired to assess the application of spectroscopy and remote sensing to characterizing and quantifying these biochemical constituents. Additional, fundamental information about the impact of phenolic constituents on vegetation spectra is needed to assess the contribution of plant phenolics to species discrimination using spectroscopy and remote sensing. Our objectives in this paper are: (1) to add to the understanding of the reflectance spectra of plant phenolic compounds, and (2) to examine leaf and canopy reflectance spectra in the 1.66 μm region for direct evidence of absorption features attributable to plant phenolics. To accomplish these objectives, we present laboratory spectra of phenolic compounds, including tannic acid and smaller compounds that form the building blocks of plant phenolics. Utilizing linear continuum removal, we use spectral feature analysis (SFA; see Kokaly et al., 2003) to examine the wavelength positions of absorption in the measured spectra and contrast these measurements with the positions and shapes of major plant constituents (lignin, cellulose, starch, and protein). We examine leaf and plant canopy spectra in available spectral libraries, and from our own measurements, to test if unique absorption features related to plant

**Table 1**
Sources of biochemical compounds and reflectance data.

| Biochemical compound | Chemical formula | Molecular weight (g/mol) | Source supplier (item#) or publication | Sample identifier |
|---|---|---|---|---|
| Phenolics | | | | |
| Phenol | $C_6H_6O$ | 94 | Sigma–Aldrich (#328111) | Phenol |
| Pyrogallol | $C_6H_6O_3$ | 126 | Sigma–Aldrich (#16040) | Pyrogallol |
| Ellagic acid | $C_{14}H_6O_8$ | 302 | Sigma–Aldrich (#E2250) | Ellagic acid |
| Gallic acid | $C_7H_6O_5$ | 170 | Sigma–Aldrich (#G7384) | Gallic acid |
| Naringenin | $C_{15}H_{12}O_5$ | 272 | Sigma–Aldrich (#N5893) | Naringenin |
| Quercetin | $C_{15}H_{10}O_7$ | 302 | Sigma–Aldrich (#Q4951) | Quercetin |
| Tannic acid | Approx. $C_{76}H_{56}O_{46}$ | ~1700 | Sigma–Aldrich (#403040) | Tannic acid-1 |
| Tannic acid | Approx. $C_{76}H_{56}O_{46}$ | ~1700 | Elvidge (1990) | Tannic acid-2 |
| Lignin, pine | No defined structure, approximately $(C_{31}H_{34}O_{11})_n$ | ~8000 | Elvidge (1990) | Lignin-1 |
| Lignin, sweetgum | No defined structure, approximately $(C_{31}H_{34}O_{11})_n$ | ~8000 | Elvidge (1990) | Lignin-2 |
| Lignin, alkali | No defined structure, approximately $(C_{31}H_{34}O_{11})_n$ | ~8000 | Sigma–Aldrich (#37095) | Lignin-3 |
| Other plant biochemical constituents | | | | |
| Cellulose | $(C_6H_{10}O_5)_n$ with β-1,4 linkages | 10,000–100,000 | Sigma–Aldrich (#C6288) | Cellulose |
| Starch, potato | Contains amylose and amylopectin; $(C_6H_{10}O_5)_n$ with α-1,4 linkages and α-1,6 branching | 10,000–1000,000 | Sigma–Aldrich (#33615) | Starch |
| Amylose, potato | $(C_6H_{10}O_5)_n$ with α-1,4 linkages | 10,000–100,000 | Sigma–Aldrich (#A0512) | Amylose |
| Protein, vegetable | Amino acids linked by peptide bonds | 11,000–120,000 (in chloroplasts) | NOW company (nutrient supplement) | Protein |

phenolics are present. Finally, we test the relationships between absorption feature parameters (e.g., depth, width, and area) and phenolic concentrations, at leaf and canopy reflectance levels.

## Materials and methods

### *Plant biochemical components*

#### *Purchased plant biochemical components*

A variety of sources were used to compile a spectral library of plant biochemical components, including measurements of chemicals purchased from chemical supply companies and spectra in publicly available spectral libraries and commercial software packages. Table 1 shows the chemical compounds, including lignin, tannic acid, and smaller phenolic compounds that are basic components of plant phenolics, such as gallic acid and ellagic acid. Many of these compounds were purchased from Sigma–Aldrich (St. Louis, Missouri, USA). Fig. 1 shows the chemical structures of the phenolic compounds. The most basic phenolic, phenol, was measured. Two flavonoids, the flavonol quercetin and the flavanone naringenin, were measured. In addition to these phenolic compounds, basic components of plant cells, cellulose, starch, and protein, were purchased and measured.

#### *Spectral measurement of plant biochemical constituents*

We measured reflectance using an artificial (tungsten halogen) light source illuminating the sample. The light source was 50 cm from the sample. The make of the spectrometers used to measure reflectance spectra was Analytical Spectral Devices (ASD; Panalytical Boulder, Colorado, USA). Numerous models of the ASD spectrometers were used. The models used and the processing methods are described in Section Spectral processing and analysis. The bare fiber optic head of the spectrometer has a 20° field of view. The fiber optic head was placed 3–10 cm from the sample at a 30 zenith angle and 90° orthogonal in azimuth to the illumination direction. The 90° orientation was used to reduce specular reflection. Because the amount of sample varied, the fiber optic head was adjusted up or down in order to ensure the field of view included only the sample material being measured. The Spectralon™ (Labsphere, North Sutton, New Hampshire, USA) white reference panel was measured at the same distance as the sample to spectrometer distance. The number of spectra recorded for each sample varied from 19 to 42. The reflectance spectra measured in this setup are termed conical-conical reflectance factors (CCRF) by Schaepman-Strub, et al. (2006).

### *Spectra of dried and fresh leaves and plant canopies*

#### *ACCP data set of spectra of dried, ground leaves and associated biochemical composition*

The NASA Accelerated Canopy Chemistry Program (ACCP) data set was compiled by an interdisciplinary team to investigate the feasibility of quantifying canopy biochemical composition from remote sensing observations (ACCP, 1994). The data set contains spectra and biochemistry for more than 30 deciduous and coniferous tree species. Prior to measurement, leaf samples were oven dried at 70 °C for 48 h, ground through a 1-mm mesh, and homogenized (Newman et al., 1994). Spectra over the range 1.1–2.5 μm were measured with NIRSystems Model 6250 and 6500 scanning monochromators (NIRSystems, Silver Springs, Maryland, USA) with a spinning sample cup module (Bolster et al., 1996; Johnson and Billow, 1996). The instruments had 2-nm sampling interval with 10-nm bandpass. The ACCP data were converted from $\log(1/R)$ to reflectance as described in Kokaly (2001). The reflectance spectra measured in this setup are termed bihemispherical reflectance (BHR) by Schaepman-Strub, et al. (2006).

Plant samples were analyzed by Newman et al. (1994) for nitrogen concentration with a PerkinElmer CHN Elemental Analyzer (PerkinElmer, Norwalk, CT, USA). Lignin and cellulose concentration were determined by a modified wood-products chemistry procedure (Newman et al., 1994). Douglas-fir samples were analyzed for nitrogen (Johnson and Billow, 1996) with a Perstorp Analytical RFA/2 continuous flow auto-analyzer (Perstorp-OI Corporation, College Station, TX, USA).

Reflectance spectra were analyzed using methods described in Section Automated SFA. Biochemical concentrations from the ACCP were used to interpret changes in the positions and shapes of phenolic absorption features when influenced by cellulose and other biochemical constituents of plants.

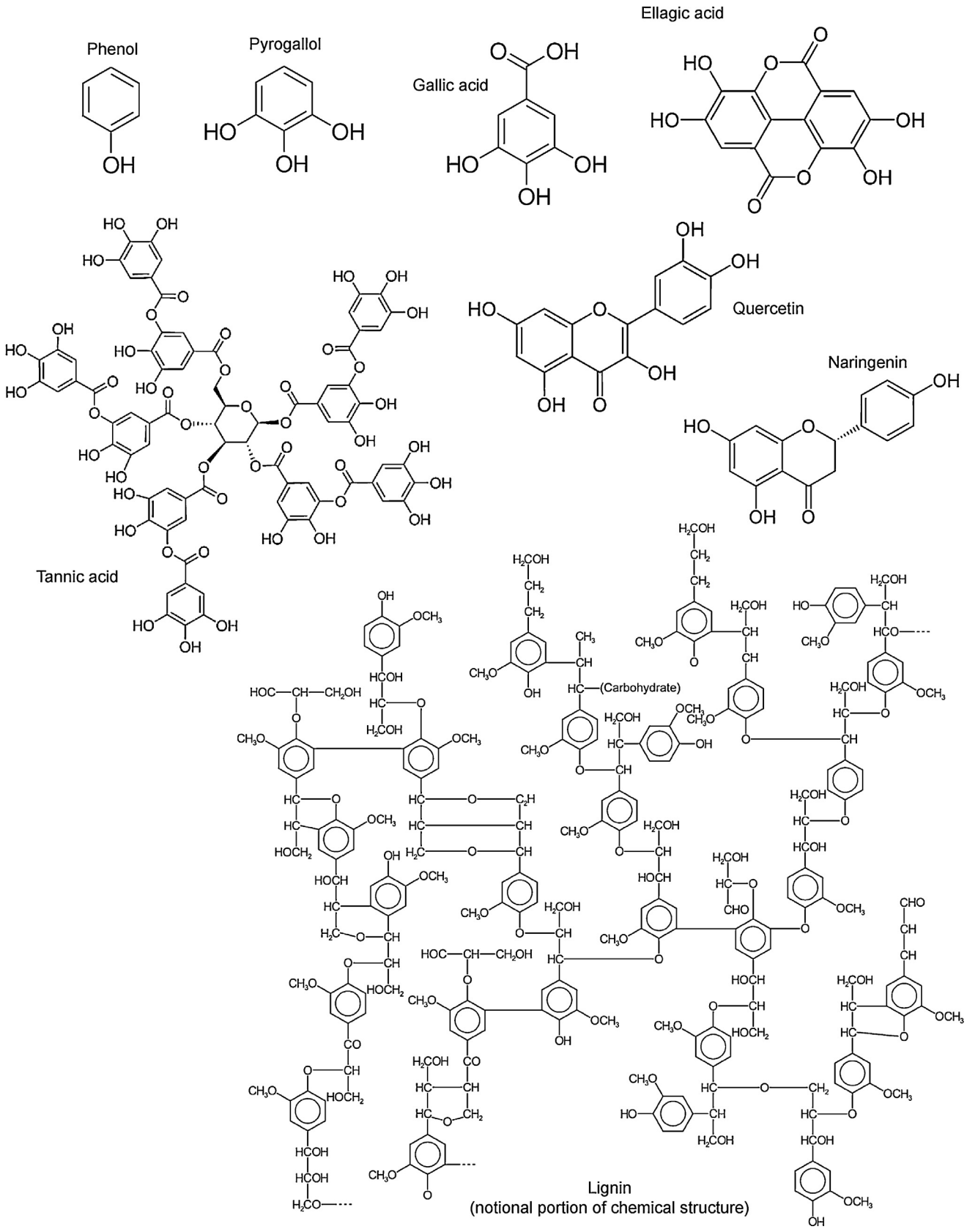


**Fig.1.** Chemical structures of phenolic compounds.

*Spectra of dry plant materials from Elvidge (1990)*

In addition to the measured spectra of materials, we used spectra from published spectral libraries in the commercially available ENVI software (Exelis Visual Information Solutions, Boulder, Colorado, USA), specifically dry plant matter from Elvidge (1990). The spectra that we analyzed are shown in Table 2. Elvidge (1990) describes the data as hemispherical reflectance spectra measured from 0.4 to 2.5 μm. The spectrometer used was a Beckman UV-5240 spectrophotometer equipped with an integrating sphere. The sampling interval of the spectrometer was reported as 1 nm in the 0.4–0.8 μm region and 4 nm from 0.8 to 2.5 μm. Bandwidths were smaller than 5 nm over most of the 0.4–1.3 μm region and between 4 nm and 16 nm over most of the 1.3–2.3 μm wavelength region (ranging from 1 nm to 28 nm overall). A halon plate was used as a reflectance standard. No information is given in Elvidge (1990) about whether spectra were left as relative reflectance or whether they were converted to absolute reflectance. The reflectance spectra measured in this setup are termed bihemispherical reflectance (BHR) by Schaepman-Strub, et al. (2006).

*Spectral measurements of dried and fresh leaves*

Reflectance spectra of dried and fresh leaves of manzanita, sumac, sagebrush, pine, fir and Douglas-fir were measured using ASD spectrometers (Table 2). Leaves were stacked in optically thick piles. The bare fiber of an ASD spectrometer was used to measure the reflectance spectra of the stacked leaves relative to a Spectralon white reference panel. The fiber optic cable was pointed at nadir (straight down) at a height of 6 cm above the leaves and moved around the area of stacked leaves during the measurement. The instrument was programmed to record 6 s averages of reflectance (thus, each recorded spectrum was an average of 60 individual measurements). The spectrometer was configured to measure 240 samples of dark current (24 s integration time) and 240 samples of white reference (24 s integration time). The number of spectra recorded for each sample varied from 15 to 31. The ASD spectrometers were used in the laboratory to measure the reflectance spectra of all samples except for manzanita, which was measured in the field (Swayze et al., 2009). The laboratory reflectance spectra are termed conical-conical reflectance factors (CCRF) by Schaepman-Strub, et al. (2006). Because sunlight was the illumination source for the manzanita spectra, these reflectance spectra are hemispherical-conical reflectance factors (HCRF), as described by Schaepman-Strub, et al. (2006). Recorded spectra were processed according to the methods in Section Spectral processing and analysis.

*Spectral measurements of plant canopies*

Reflectance spectra of plant canopies of manzanita, sumac, chokecherry, sagebrush, juniper, and pine were measured using ASD spectrometers, see Table 2. These reflectance spectra were measured with an ASD spectrometer relative to a Spectralon reference panel. The bare fiber of the spectrometer was used to measure the reflectance spectra of a single manzanita bush. The fiber optic cable was pointed at nadir (straight down) at approximately shoulder height above each plant that was measured. The instrument was programmed to record 6 s averages of reflectance (thus, each recorded spectrum was an average of 60 individual measurements). The spectrometer was configured to measure 240 samples of dark current (24 s integration time) and 240 samples of white reference (24 s integration time). The number of spectra recorded for each sample varied from 5 to 16. Recorded spectra were processed according to the methods in Section Spectral processing and analysis. Because sunlight was the illumination source for the plant spectra, these reflectance spectra are hemispherical-conical reflectance factors (HCRF), as described by Schaepman-Strub, et al. (2006).

*Tea leaf and canopy spectral measurements and phenolic concentrations*

Reflectance spectra of dried and fresh leaves and plant canopies of tea (*Camellia sinensis*) were measured by Bian et al. (2013). Fifty-six leaf samples and forty-eight tea canopies were measured. The spectral measurements are described by Bian et al. (2013) and briefly summarized here. Fresh tea leaves were measured using an ASD FieldSpec Pro FR spectrometer with the bare fiber over a circular measurement area of 10 cm diameter. Within this measurement area, an optically dense pile of leaves (more than 200 leaves in more than 10 layers) was placed on top of a black thick cardboard. Spectra were measured relative to a Spectralon white reference panel. Each recorded spectrum was an average of 10 measurements (1 s integration time). Nine recordings were made of each leaf pile. In between each recording, the leaves on the tray were randomly rearranged. The tray was rotated horizontally 120° after every three recordings. The nine recordings were averaged and converted to absolute reflectance. Subsequently, the reflectance spectra were corrected for detector offsets according to the methods in Section Spectral processing and analysis.

To prepare dried, powdered tea, the fresh leaves were placed in an oven for more than 10 h at 80 °C. Dried leaves were ground using an electric mill and passed through a sieve with a mesh width of 75 microns. The ASD FieldSpec Pro FR spectrometer with a 5° foreoptic was used to measure a 1 cm area of the tea powder (from a height of 12 cm above a circular area of 10 cm of tea powder). The thickness of the layer of tea powder in the dark container was 1 cm. The spectrum of each pile of tea powder was recorded three times, where each recording had an integration time of 1 s. Spectra were measured relative to a Spectralon white reference panel. For each pile, recordings were averaged and converted to absolute reflectance. Subsequently, the reflectance spectra were corrected for detector offsets according to the methods Section Spectral processing and analysis. The laboratory arrangements for measuring tea reflectance spectra resulted in conical-conical reflectance factors (CCRF) as described by Schaepman-Strub, et al. (2006).

The spectral measurements of tea canopies were carried out between 10:30 and 13:00 on cloud-free, sunny days in September, 2008. The bare fiber optic of the spectrometer was approximately 10–20 cm above the top of the plants, with a measured area of approximately 15–60 $cm^2$. Soil background was less than 1%. Six points over each tea bush were measured with 1 s integration time (thus, each recording was the average of ten individual sample measurements). The Spectralon white reference panel was measured between each recording of canopy spectra to allow for changing illumination. The measurements from four tea bushes were considered a single observation. The spectra from the four plants were averaged and converted to absolute reflectance. Subsequently, the reflectance spectra were corrected for detector offsets according to the methods in Section Spectral processing and analysis. Because sunlight was the illumination source for the tea plants these reflectance spectra are hemispherical-conical reflectance factors (HCRF), as described by Schaepman-Strub, et al. (2006). With the distinctions between measurement setups and reflectance terminology noted in the subsections of this Materials and methods Section, the generic term reflectance is used in the rest of this paper.

Wet chemistry analysis of dried and ground tea powder was carried out in the laboratory as described by Bian et al. (2013). Standard wet chemistry methods were used to determine the concentrations of total tea polyphenols using the Folin-Ciocalteu method with the solution absorbance read at 765 nm (Ainsworth and Gillespie, 2007).

**Table 2**
Plant materials measured.

| Measurement level | Sample identifiers | Common name | Scientific name | Source location or publication | Description |
|---|---|---|---|---|---|
| Leaves, dry | Manzanita1-B | Bigberry manzanita | *Arctostaphylos glauca* | Elvidge (1990) | Bark, red |
| | Manzanita1-LD | Bigberry manzanita | *Arctostaphylos glauca* | Elvidge (1990) | Leaves, dried |
| | Sage-LD1 | Big sagebrush | *Artemisia tridentata* Nutt. | Yellowstone National Park (NP), Wyoming, USA | Leaves, dried |
| | Sage-LD2 | Big sagebrush | *Artemisia tridentata* Nutt. | Elvidge (1990) | Leaves, senesced |
| | Pine1-LD | Whitebark pine | *Pinus albicaulis* Engelm. | Yellowstone NP, Wyoming, USA | Needles, dried |
| | Pine2-LD | Lodgepole pine | *Pinus contorta* Douglas ex Loudon | Yellowstone NP, Wyoming, USA | Needles, dried, light green |
| | Fir-LD | Subalpine fir | *Abies lasiocarpa* (Hook.) Nutt. | Yellowstone NP, Wyoming, USA | Needles, dried |
| | Dougfir-LD | Douglar fir | *Pseudotsuga menziesii* | Yellowstone NP, Wyoming, USA | Needles, dried |
| Leaves, fresh | Manzanita1-LF | Bigberry manzanita | *Arctostaphylos glauca* | Elvidge (1990) | Leaves, fresh |
| | Manzanita2-LF | White stickyleaf manzanita | *Arctostaphylos viscida* Parry | El Dorado county, California, USA | Leaves, fresh |
| | Sumac-LF | Smoothbark sumac | *Rhus glabra* L. | Dinosaur Ridge, Colorado, USA | Leaves, fresh |
| | Sage-LF | Big sagebrush | *Artemisia tridentata* Nutt. | Arches NP, Utah, USA | Leaves, fresh |
| | Pine1-LF | Whitebark pine | *Pinus albicaulis* Engelm. | Yellowstone NP, Wyoming, USA | Needles, fresh |
| | Pine2-LF | Lodgepole pine | *Pinus contorta* Douglas ex Loudon | Yellowstone NP, Wyoming, USA | Needles, fresh |
| | Fir-LF | Subalpine fir | *Abies lasiocarpa* (Hook.) Nutt. | Yellowstone NP, Wyoming, USA | Needles, fresh |
| Plants | Manzanita2-P1 to -P6 | White stickyleaf manzanita | *Arctostaphylos viscida* Parry | El Dorado county, California | Six different shrubs |
| | Sumac-P | Sumac | *Rhus* spp. | Theodore Roosevelt NP, North Dakota, USA | Shrub |
| | Chokecherry-P | Chokecherry | *Prunus virginiana* L. | Theodore Roosevelt NP, North Dakota, USA | Shrub |
| | Sage-P1 and -P2 | Big sagebrush | *Artemisia tridentata* Nutt. | Lefthand Creek, Wyoming, USA | Shrub |
| | Juniper-P | Juniper | *Juniperus* spp. | Lefthand Creek, Wyoming, USA | Shrub |
| | Pine3-P | Limber pine | *Pinus flexilis* James | Lefthand Creek, Wyoming, USA | Small tree |
| Tea | Tea-LD01 to -LD56 | Tea | *Camellia sinensis* (L.) Kuntze | Bian et al. (2013) | Dried and ground leaves |
| | Tea-LF01 to -LF56 | Tea | *Camellia sinensis* (L.) Kuntze | Bian et al. (2013) | Thick stacks of leaves |
| | Tea-P01 to -P48 | Tea | *Camellia sinensis* (L.) Kuntze | Bian et al. (2013) | Bushes |

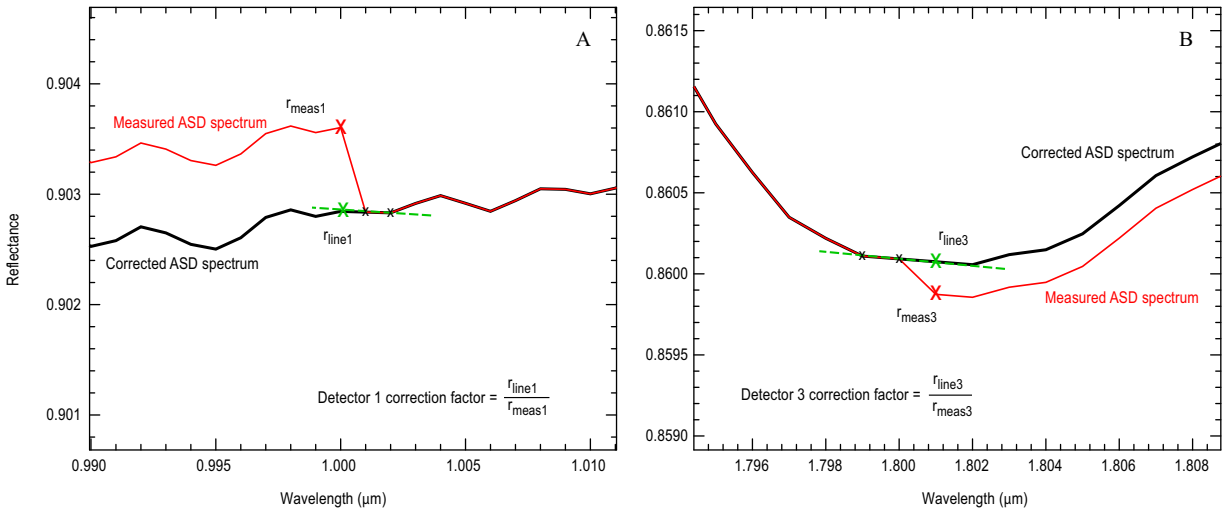


**Fig. 2.** Example of offset correction for ASD detectors: (A) detector 1; and (B) detector 3.

*Spectral processing and analysis*

Spectra were processed and analyzed using a freely available spectral analysis package written in Interactive Data Language (IDL; Exelis Visual Information Solutions, Boulder, Colorado, USA). The USGS Processing Routines in IDL for Spectroscopic Measurements (PRISM) software has been described by Kokaly (2011) and is publicly available. When used to average ASD spectra, PRISM allows the user to correct the offsets between detectors and to convert the data to absolute reflectance. PRISM functions for continuum removal and spectral feature analysis were also used in this study.

*Correcting detector offsets*

Because the spectra used in this study were collected at different field sites over the course of more than ten years, a variety of ASD field spectrometer models were used, including the FullRange (FR), FieldSpec Pro FieldSpec3, and FieldSpec4 models. These spectrometers all span the wavelength range of 0.35–2.50 μm using three detectors, with reflectance reported every 1 nm. Generally, the detectors cover the wavelength ranges 0.350–1.000, 1.001–1.800, and 1.801–2.500 μm. The exact splice positions between detectors vary by instrument and depend on detector performances and manufacturer settings. Offsets between detectors arise from the spectrometer design, where optical fibers lead to different detectors. Although the fibers are randomized in the fiber optic cable, there is still the possibility that fibers leading to the different detectors may, on average, be viewing slightly different parts of a measured surface. This will be most apparent when the fiber optic head is close to the measured surface, the sample is heterogeneous, and the fiber optic head is held in a static position.

PRISM applies simple multiplicative factors to correct the detector offsets. The second detector has been observed to be more stable at the end points of its wavelength coverage, compared to the other detectors. As a result, the first and third detectors are adjusted to be consistent with the middle detector. A linear extrapolation is made from the last two channels of the stable detector to the end channel of the detector to be adjusted. The multiplicative factor is calculated by dividing the extrapolated reflectance value by the recorded reflectance value. The factor is applied to all channels of the detector being adjusted. Fig. 2a and b illustrate the calculation of the correction factors.

*Conversion from relative reflectance to absolute reflectance*

Spectrometer data collection commonly involves a white reference panel. The energy reflected off the reference is used as a proxy for the energy illuminating the sample material or target area. However, reference panels are not completely reflective. Converting the data to absolute reflectance removes the distorting influence caused by absorption of energy by the reference panel.

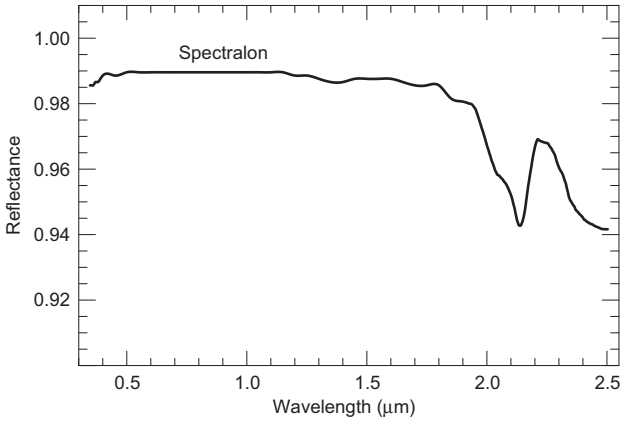


**Fig. 3.** Reflectance spectrum of Spectralon.

In this study, absolute reflectance ($R$) as a function of wavelength ($\lambda$) was obtained by multiplying the reflectance measurement made relative to Spectralon ($R_{rel}$) by the reflectance of Spectralon:

$$R(\lambda) = R_{rel}(\lambda) \times R_{Spectralon}(\lambda) \quad (1)$$

The reflectance of Spectralon was determined at the USGS Spectroscopy Lab in Denver (G. Swayze, unpublished data) using the procedure described for halon in Clark et al. (1990). As the reflectance spectrum of Spectralon shows (Fig. 3), the contamination of the panel is very small over most wavelengths. However, there is a significant absorption by Spectralon in the wavelengths between 1.95 and 2.21 μm and at wavelengths greater than 2.25 μm. If this influence of Spectralon is not removed, the "relative reflectance spectrum" of a sample will be distorted for wavelengths greater than 1.95 μm (Clark et al., 2002). Fig. 4a shows an example of measurements of leaves of sagebrush made with an ASD spectrometer. Fig. 4b shows the averaged, offset-corrected spectrum converted to absolute reflectance, along with one of the measured spectra for comparison.

*Continuum removal*

Continuum removal is used to isolate and analyze features in reflectance spectra (see Clark and Roush, 1984; Kokaly and Clark,

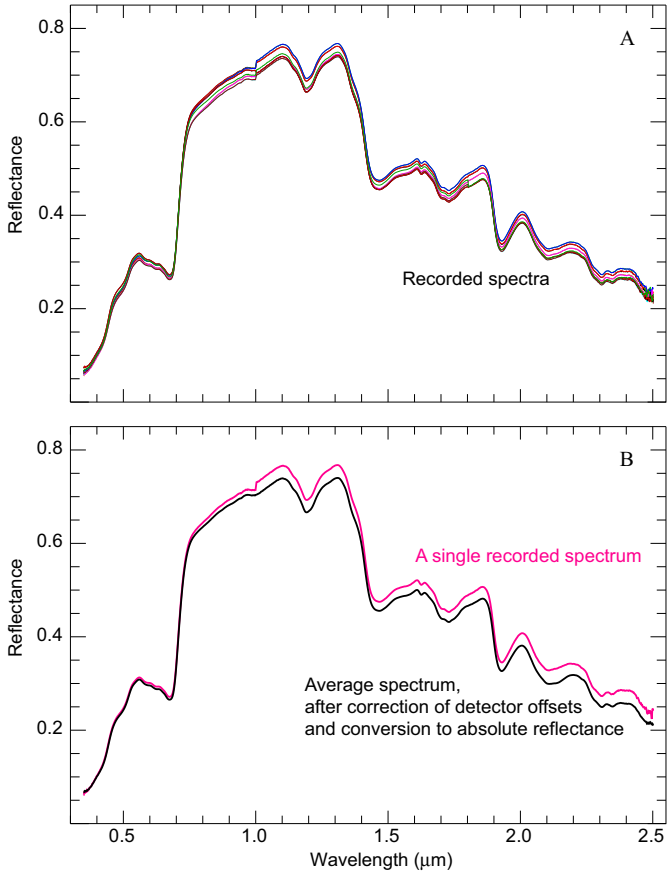


**Fig. 4.** Comparison of ASD spectra: (A) relative reflectance with uncorrected offsets; and (B) averaged, absolute reflectance spectrum with offsets corrected.

1999). Continuum removal, also referred to as baseline normalization, has been commonly used in laboratory infrared spectroscopy. This technique has been applied to spectra as part of analyses to map the distribution of minerals and vegetation (Clark et al., 1990; Mustard and Sunshine, 1999; Clark et al., 2003; Kokaly et al., 2003; Kokaly, 2011). The continuum is an estimate of the other absorptions present in the spectrum, not including the one of interest (Clark, 1999; Clark and Roush, 1984). In that sense, continuum removal is most often performed on absorption features.

The continuum is defined by the line connecting the continuum endpoints (Fig. 5a). The continuum endpoints are the channels at the high points on the left and right sides of the absorption feature ($C_1$ and $C_2$, respectively). The values of the continuum-removed spectrum ($R_C$) are calculated by dividing the original reflectance values ($R$) by the corresponding values of the continuum line ($R_L$) for all the channels in the wavelength region ($\lambda_1$ to $\lambda_2$) between the endpoints of the absorption feature:

$$R_C(\lambda) = \frac{R(\lambda)}{R_L(\lambda)} \quad (2)$$

*SFA and calculating the feature center*

The continuum-removal process allows the separation of the absorption feature of interest from the spectral influence of background materials. The continuum-removed feature can then be further analyzed to compute parameters that describe the absorption feature, such as the central wavelength position, the feature depth, and the feature width (see Kokaly, 2011). Collectively, this has been termed spectral feature analysis (SFA; Kokaly et al., 2003).

Here, we call the central wavelength of the absorption the feature center. In previous studies, this has been termed band center.

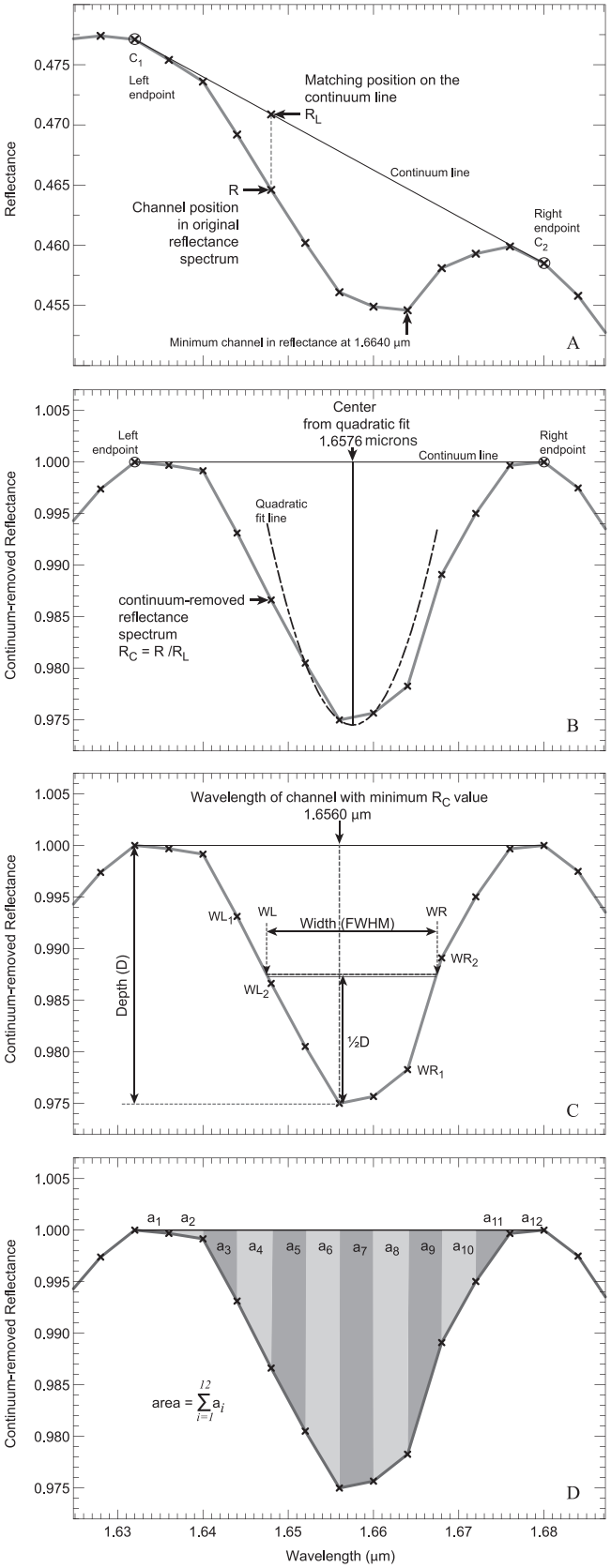


**Fig. 5.** Spectral feature analysis: (A) continuum endpoints and continuum line; (B) feature center position determined by quadratic fit to the minimum channel in the continuum-removed spectrum and one channel on each side; (C) feature depth and width (full-width at half-maximum); and (D) feature area, calculated by summing the individual areas between the continuum line and channels in the continuum-removed feature.

We prefer the term feature center to avoid confusion of band center with the common usage of the word band to describe a channel of a multispectral sensor. There are many ways to characterize the feature center, including, the wavelength position of the minimum channel in the continuum-removed feature, polynomial functions fitted to the band minimum channel and channels on each side (Clark, 1993; Cameron et al., 1982; Savitzky and Golay, 1964), and center of gravity methods (Choquette et al., 1998; Cameron et al., 1982).

A standard technique for determining the feature center has been the fitting of a quadratic function to the band minimum channel and one channel on either side (Clark, 1993). As opposed to the use of the band minimum channel, the quadratic fit is not tied to the sampling positions of a single channel in a spectrometer and somewhat resistant to the effect of noise (Cameron et al., 1982). This methodology has been adopted in newer software tools (Kokaly, 2011; van Ruitenbeek et al., 2014). In this paper, we report feature centers using the quadratic fit approach in PRISM which utilizes the singular value decomposition least-squares fitting algorithm (SVDFIT) of IDL. Fig. 5b shows an example of quadratic fitting, using PRISM, to establish the central wavelength of an absorption feature.

*Feature depth and area*

The depth ($D$) of an absorption feature is calculated as the difference between the continuum line and the minimum value in the continuum-removed spectral feature:

$$D = 1.0 \min(R_C) \quad (3)$$

The feature width is calculated as the full-width at half-maximum (FWHM) of the feature depth. The width of a line at half-maximum ($\frac{1}{2}D$) is calculated using the intersection of the half-maximum line with line segments connecting the spectrometer channels. On the left of the center line, the channels that fall above and below the half maximum value ($WL_1$ and $WL_2$, respectively) are used to establish the left wavelength value of the FWHM line (WL). On the right of the center line, the channels that fall below and above the half maximum value ($WR_1$ and $WR_2$, respectively) are used to establish the right wavelength value of the FWHM line (WR). Examples of these values are illustrated on Fig. 5c. Linear interpolation is used to calculate the WL and WR values. The feature width defined in this manner is termed FWHM and is simply computed as:

$$\mathrm{FWHM} = \mathrm{WR} - \mathrm{WL} \quad (4)$$

FWHM has units of wavelength. In this study we used nanometers (nm) because the features had widths of a magnitude that were conveniently expressed in this format.

The feature area is calculated using all the channels that fall within the continuum endpoints ($C_1$ and $C_2$). The individual areas below the continuum line are calculated and summed to calculate the total area of the feature (Fig. 5d).

*Automated SFA*

PRISM has a function for automated spectral feature analysis (Kokaly, 2011). With this function, the user establishes the initial continuum endpoints and the set of spectra to be analyzed. The PRISM software applies continuum removal to each spectrum and derives the spectral feature parameters (e.g., center, depth, width, area, etc.). PRISM performs continuum removal twice and reports the feature parameters for: (1) the initial set of continuum endpoints; and (2) an automatically adjusted set of continuum endpoints. The initial endpoint selection is referred to as the fixed endpoints. PRISM looks for better continuum endpoints on both sides of the absorption feature, by searching for nearby channels that have continuum-removed values higher than the initial endpoints. The new endpoint channels are referred to as the adjusted endpoints. The searching is done within a restricted number of channels to either side of each endpoint. Because many studies have indicated that reflectance in the 1.66 μm region is highly correlated to phenolic concentrations in plant matter, the automated spectral analysis was applied to this portion of leaf and plant spectra. The initial continuum endpoints and ranges for adjusted endpoints are shown in Table 3 for the different spectral data sets.

In this paper, the descriptive parameters (center, depth, width, and area) are reported for the adjusted continuum endpoints. However, feature parameters from both the fixed and adjusted endpoints were used in regression analysis with tea phenolic concentrations. Also, because their continuum endpoints varied so greatly and there were just a few samples, automated spectral feature analysis was not applied to the spectra of the biochemical compounds. Instead, a custom selection of endpoints was done using the interactive continuum removal function of PRISM.

*ASD wavelength and bandpass evaluation*

The wavelength position and bandpass performance of the ASD spectrometers were evaluated using wavelength calibration materials with narrow absorption features. Bandpass is the wavelength interval over which each channel is sensitive. The evaluation procedure is described in the PRISM software user's guide (Kokaly, 2011). This procedure involves the measurement of one-pass transmission through three reference materials: a NIST SRM 2035 (Choquette et al., 1998), which is a rare-earth doped glass, a praseodymium-doped glass, and a Mylar plastic sheet. Because the absorption features of these materials are narrow, transmission measurements made on higher resolution spectrometers (those with smaller sampling interval and bandpass) can be convolved and compared to the ASD measurements. Kokaly (2011) describes the process of convolving and comparing the narrow absorption features to estimate the average ASD bandpass for each detector range. With the bandpass performance characterized, Kokaly (2011) describes how the center wavelength positions of absorption features can be calculated and compared to check for and correct for shifts in spectrometer wavelengths. The standard resolution ASD spectrometers used in this study had bandpass values, on average, of 5 nm, 11 nm, and 11 nm, respectively for the three detectors. A high resolution FieldSpec3 was used to measure many of the phenolic compounds. This instrument had average bandpass values of 4 nm, 9 nm, and 9 nm, for its three detectors.

*Linear regression with phenolic concentrations*

Simple regression was used to test if the 1.66 μm absorption feature parameters are linearly related to phenolic concentrations in tea leaves. First, the automated spectral feature analysis was applied to the tea spectra. The LINEST function of Excel (Microsoft; Redmond, Washington, USA) was used to relate feature depths, widths, and areas, separately, with the phenolic concentrations. Independent regressions were performed with the dry, fresh and canopy data sets. Regressions were calculated using parameters derived from both the initial continuum endpoint selections and the automatically adjusted endpoints. Four parameters were used to evaluate the regression results, the coefficient of determination ($r^2$), the $F$ statistic, the root-mean square error (RMSE) between actual and predicted values, and the relative RMSE (rRMSE; the RMSE divided by the sample mean, expressed as a percentage).

## Results

*Spectra of phenolic compounds*

Reflectance spectra of phenolic compounds are shown in Fig. 6. At wavelengths short ward of 1.0 μm, the spectra have slowly

**Table 3**
Initial and adjusted continuum endpoints for SFA of plant materials.

| Data set | Left continuum endpoint | | Right continuum endpoint | |
|---|---|---|---|---|
| Subset | Wavelength of initial channel (μm) | Wavelength range of adjusted endpoints (μm) | Wavelength of initial channel (μm) | Wavelength range of adjusted endpoints (μm) |
| Dried leaves | | | | |
| Manzanita | 1.634 | 1.632–1.636 | 1.680 | 1.680–1.692 |
| Sage | 1.610 | 1.608–1.611 | 1.640 | 1.640 |
| Pine/fir/Douglas-fir | 1.624 | 1.622–1.627 | 1.644 | 1.642–1.644 |
| Fresh leaves | | | | |
| Manzanita | 1.640 | 1.636–1.643 | 1.678 | 1.676–1.680 |
| Sumac | 1.636 | – | 1.676 | – |
| Sage | 1.613 | – | 1.648 | – |
| Pine/fir | 1.624 | 1.622–1.628 | 1.642 | 1.642–1.644 |
| Plant canopies | | | | |
| Manzanita | 1.646 | 1.644–1.646 | 1.681 | 1.680–1.681 |
| Sumac | 1.646 | – | 1.673 | – |
| Chokecherry | 1.655 | – | 1.676 | – |
| Sage | 1.617 | 1.617 | 1.642 | 1.641–1.644 |
| Pine/juniper | 1.621 | 1.620–1.623 | 1.646 | 1.644–1.647 |
| ACCP dried leaves | | | | |
| Red maple | 1.634 | 1.634–1.640 | 1.680 | 1.678–1.684 |
| Sugar maple | 1.650 | 1.644–1.652 | 1.676 | 1.672–1.682 |
| White birch | 1.650 | 1.644–1.654 | 1.676 | 1.672–1.682 |
| Red oak | 1.652 | 1.650–1.658 | 1.674 | 1.670–1.680 |
| White oak | 1.652 | 1.652–1.656 | 1.674 | 1.672–1.676 |
| White pine | 1.652 | 1.652–1.658 | 1.674 | 1.674–1.680 |
| Red spruce | 1.652 | 1.652–1.656 | 1.674 | 1.670–1.680 |
| Tea | | | | |
| Dried leaves | 1.649 | 1.642–1.650 | 1.679 | 1.676–1.687 |
| Fresh leaves | 1.652 | 1.646–1.658 | 1.671 | 1.666–1.676 |
| Plant canopies | 1.648 | 1.646–1.654 | 1.671 | 1.661–1.674 |

changing shapes, characterized by absorption features centered in the ultraviolet (UV). The long ward edges (wings) of the UV absorptions extend into the visible (VIS) and near-infrared (NIR). The wing of the UV extends further into the NIR for the larger molecules (tannic acids and lignins) compared to the smaller molecules (e.g., pyrogallol and gallic acid). Increasing conjugation of carbon bonds, that is, increasing the number of linkages of carbon in alternating single and double bond arrangements, can lead to such extension of the UV absorption (Schanda, 1986).

From 1 to 1.5 μm, the phenolics exhibit a small absorption feature centered near 1.13 μm. The feature is stronger (greater depth of absorption) in phenol, pyrogallol, and gallic acid and weaker in tannins). Pyrogallol and gallic acid have weak absorption features in the 1.25–1.30 μm region, which are only slightly evident for ellagic acid and tannins. The larger phenolic compounds exhibit an absorption feature centered near 1.47 μm, arising from the O—H bonds in their structures.

All the spectra of the measured compounds have an absorption featured centered near 1.66 μm. This feature shifts slightly in wavelength position (Table 4). While most of the phenolic compounds have a narrow feature (width less than 42 nm), the lignin feature is centered at a slightly longer wavelength, 1.67 μm, and is much broader (82–104 nm wide). The lignin absorption has an asymmetric shape, with more of the absorption area on the long wavelength side of the feature center.

In the 2.0–2.5 μm region, all spectra exhibit overlapping absorptions about a central wavelength near 2.14 μm. The position of strongest absorption generally shifts from a shorter wavelength for larger compounds (2.137 and 2.144 μm for tannic acid-1 and lignin-1, respectively) to longer wavelength in the smaller compounds (2.141 μm for gallic acid, 2.147 μm for phenol, 2.158 μm for ellagic acid, and 2.186 μm for pyrogallol). As noted for other features, the spectral variations are sharper and more complex in the small compounds compared to the broad, smoothly varying features in the tannin and lignin spectra.

Lignin exhibits a broad absorption feature centered near 2.27 μm; other phenolic compounds do not have strong absorption near this position. Ellagic acid has the nearest absorption; however, it is a weak absorption feature centered near 2.28 μm.

**Table 4**
Feature parameters for absorptions near 1.66 μm.

| Phenolic compound | Center (μm) | Depth | Width (nm) | Area (nm) |
|---|---|---|---|---|
| Phenol | 1.676 | 0.4847 | 37.7 | 20.598 |
| Pyrogallol | 1.671 | 0.3737 | 31.1 | 22.740 |
| Ellagic acid | 1.667 | 0.1635 | 173.9 | 25.247 |
| Gallic acid | 1.659 | 0.0832 | 14.8 | 1.466 |
| Naringenin | 1.656 | 0.1102 | 41.7 | 5.988 |
| Quercetin | 1.659 | 0.0420 | 41.3 | 1.802 |
| Tannic acid-1 | 1.657 | 0.1070 | 28.3 | 3.537 |
| Tannic acid-2 | 1.653 | 0.0820 | 24.5 | 2.226 |
| Lignin-1 | 1.669 | 0.0392 | 91.8 | 3.951 |
| Lignin-2 | 1.670 | 0.0397 | 82.4 | 3.212 |
| Lignin-3 | 1.677 | 0.0815 | 104.7 | 8.063 |

*Spectra of basic plant biochemical constituents*

Fig. 7 shows the spectra of lignin and tannic acid plotted with some of the basic plant constituents. Cellulose, starch and amylose, all chemically similar, have spectra comparable to one another. They have major absorption features centered near 1.77 and 2.10 μm, and doublet absorptions with feature centers near 2.27 and 2.33 μm. These features do vary slightly between cellulose and amylose/starch. Protein has absorption features centered near 1.73, 2.05, and 2.17 μm, and a doublet feature with centers near 2.23 and 2.35 μm. All spectra exhibit hydroxyl-related absorption features near 1.49 and 1.93 μm.

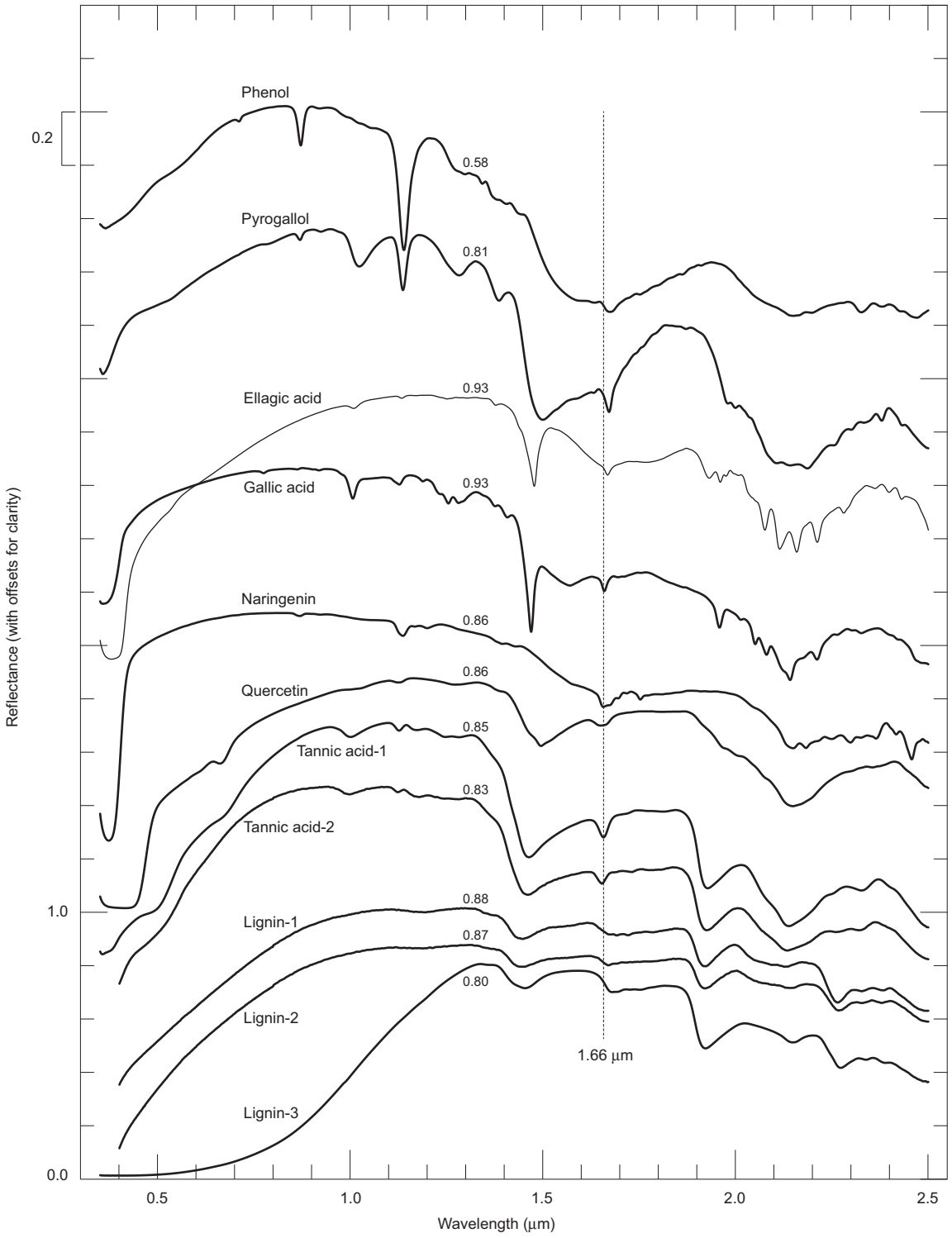


**Fig. 6.** Reflectance spectra of phenolic compounds (see Table 1 for sample descriptions). Spectra are offset for clarity. From bottom to top spectrum, the offset values added to spectra are 0.0, 0.0, 0.15, 0.6, 0.7, 1.0, 1.2, 1.7, 1.9, 2.6, and 3.2. The original reflectance values for channels at 1.3 μm are labeled next to each spectrum.

While tannic acid and the other plant phenolics have absorption features near 1.66 μm, cellulose, starch, and amylose have no absorption feature in this area and show a peak in reflectance. The closest absorption features in these compounds are weak features near 1.70 μm. Protein also has a peak in reflectance near 1.66 μm. The closest absorption features in the measured protein are weak absorptions centered near 1.58 and 1.69 μm.

*Spectra of leaves in the ACCP data set*

PRISM's automated continuum removal/spectral feature analysis was run on the ACCP spectra to detect and characterize absorption features near 1.66 μm. The results show some consistent trends in wavelength position as a function of species (Table 5). Red maple and sugar maple were both found to have a

**Table 5**
Feature parameters for absorptions near 1.66 μm and in the ACCP samples and average chemistry.

| Common name/ scientific name | # With feature of total # | Feature parameters | | | | | | | | Chemical concentrations (% by dry weight) | | | | | | | |
|---|---|---|---|---|---|---|---|---|---|---|---|---|---|---|---|---|---|
| | | Center (μm) | | Depth | | Width (nm) | | Area (nm) | | Nitrogen | | Cellulose | | Lignin | | Lignin: cellulose | |
| | | Avg. | (std. dev.) | Avg. | (std. dev.) | Avg. | (std. dev.) | Avg. | (std. dev.) | Avg. | (std. dev.) | Avg. | (std. dev.) | Avg. | (std. dev.) | Avg. | (std. dev.) |
| Red maple | 91 | 1.6587 | | 0.0237 | | 19.9 | | 0.487 | | 1.6 | | 30.3 | | 18.2 | | 0.60 | |
| *Acer rubrum* L. | of 93 | | (0.0003) | | (0.0058) | | (0.8) | | (0.139) | | (0.3) | | (2.7) | | (1.5) | | (0.08) |
| Sugar maple | 27 | 1.6613 | | 0.0040 | | 13.8 | | 0.063 | | 2.1 | | 39.7 | | 17.5 | | 0.44 | |
| *Acer saccharum* Marsh. | of 29 | | (0.0006) | | (0.0031) | | (2.5) | | (0.060) | | (0.3) | | (3.9) | | (1.2) | | (0.06) |
| White birch | 25 | 1.6629 | | 0.0038 | | 14.2 | | 0.060 | | 2.0 | | 34.1 | | 21.6 | | 0.63 | |
| *Betula papyrifera* Marsh. | of 30 | | (0.0010) | | (0.0026) | | (2.6) | | (0.049) | | (0.4) | | (2.6) | | (2.1) | | (0.07) |
| Red oak, northern | 37 | 1.6642 | | 0.0016 | | 12.1 | | 0.021 | | 2.4 | | 41.7 | | 26.1 | | 0.63 | |
| *Quercus rubra* L. | of 90 | | (0.0011) | | (0.0008) | | (2.3) | | (0.015) | | (0.3) | | (2.5) | | (2.2) | | (0.08) |
| White oak | 19 | 1.6640 | | 0.0008 | | 9.4 | | 0.008 | | 2.6 | | 43.6 | | 21.7 | | 0.50 | |
| *Quercus alba* L. | of 29 | | (0.0004) | | (0.0004) | | (1.0) | | (0.005) | | (0.2) | | (2.4) | | (2.2) | | (0.07) |
| White pine, eastern | 38 | 1.6664 | | 0.0019 | | 13.3 | | 0.026 | | 1.6 | | 38.5 | | 26.5 | | 0.69 | |
| *Pinus strobus* L. | of 40 | | (0.0018) | | (0.0006) | | (2.4) | | (0.011) | | (0.2) | | (3.1) | | (1.8) | | (0.06) |
| Red spruce | 49 | 1.6688 | | *0.0043* | | 15.4 | | 0.066 | | 0.9 | | 40.2 | | 26.9 | | 0.67 | |
| *Picea rubens* Sarg. | of 49 | | (0.0011) | | (0.0014) | | (1.1) | | (0.022) | | (0.1) | | (2.3) | | (2.2) | | (0.05) |

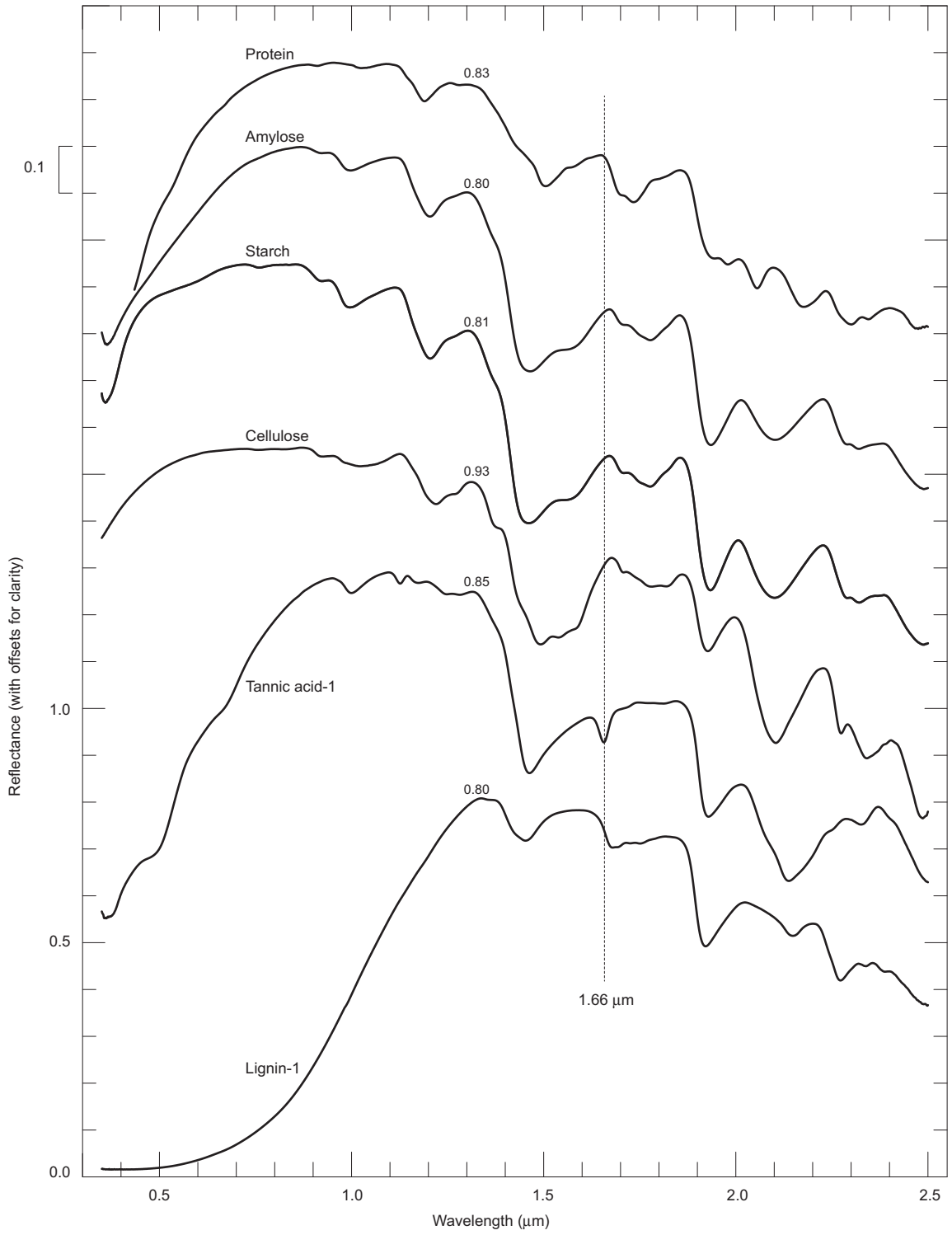


**Fig.7.** Reflectance spectra of major plant constituents and tannic acid (see Table 1 for sample descriptions). Spectra are offset for clarity. From bottom to top spectrum, the offset values added to spectra are 0.0, 0.4, 0.5, 1.0, 1.3, and 1.5. The original reflectance values for channels at 1.3 μm are labeled next to each spectrum.

high percentage of spectra with absorption features at the 1.66 μm position. The feature was much deeper, on average, for red maple compared to sugar maple.

Fig. 8 shows example reflectance spectra for the species shown in Table 5. Absorption features near 1.66 μm are clearly evident on the shoulder of the broad 1.72 μm features for the red maple, sugar maple, white birch and red oak spectra. It is weakly present in the spectrum of the white oak sample. It appears to be absent from the white pine and red spruce spectra. Table 5 shows that, on average, the feature becomes weaker and shifts position from 1.659 μm in red maple to 1.664 μm in red oak. The automated spectral feature analysis reports a weak feature, shifted to longer wavelengths near 1.67 μm, for white pine and red spruce samples.

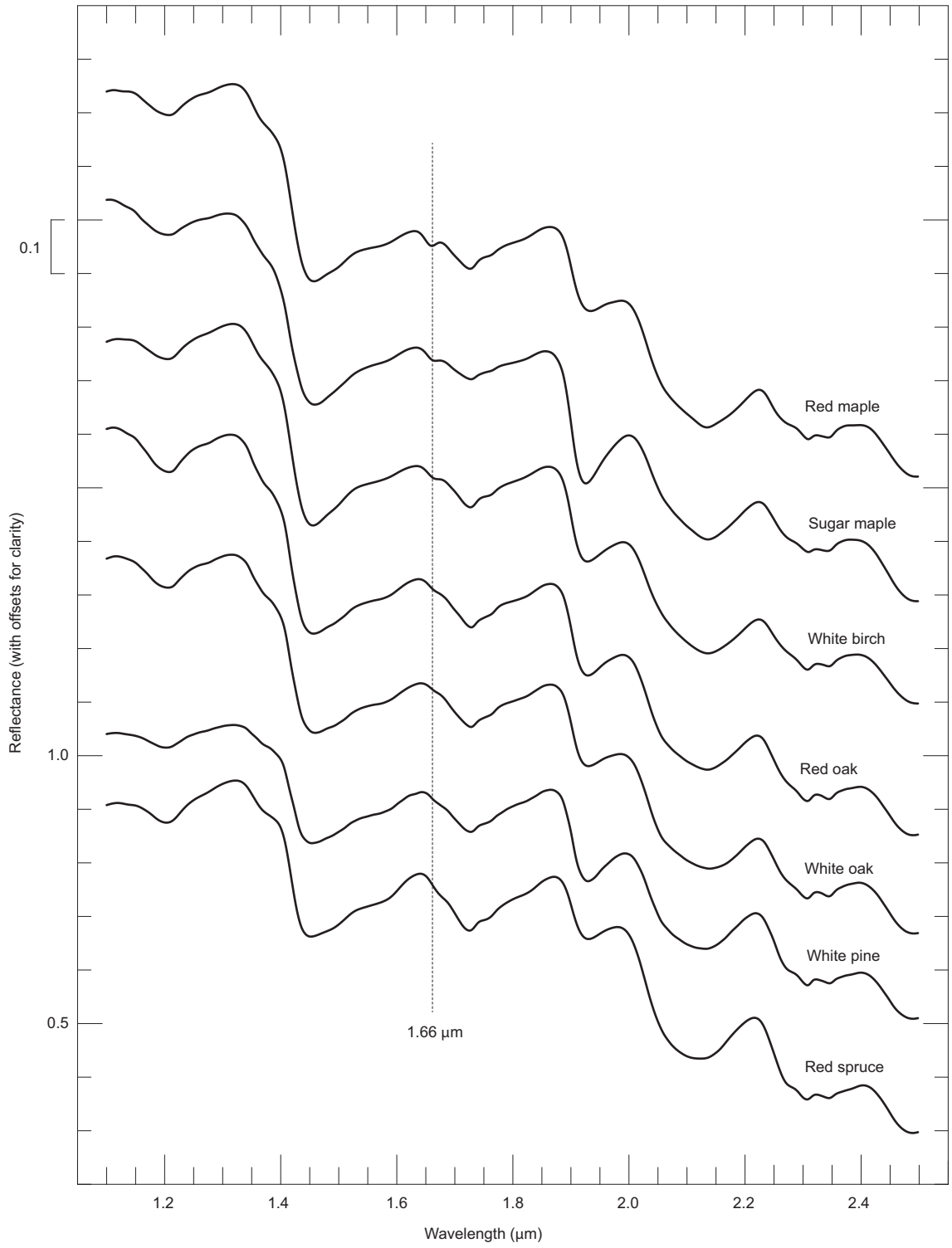


**Fig. 8.** Reflectance spectra of samples from the ACCP dry leaf data set. Spectra are offset for clarity. From bottom to top spectrum, the offset values added to spectra are 0.0, 0.2, 0.3, 0.5, 0.8, 0.9, and 1.2.

*Spectra of dry plant matter*

The spectra of manzanita bark (manzanita1-B) and dried manzanita leaves (manzanita1-LD) show an absorption feature centered near 1.66 μm (Fig. 9). Table 6 shows that the feature in bark is at 1.662 μm and in the leaves the feature is at 1.658 μm. Weaker spectral features were found near this position in the sagebrush and conifer spectra; however, they are centered at shorter wavelength positions compared to manzanita (at wavelengths less than 1.636 μm, see Fig. 9 and Table 6).

*Spectra of fresh leaves*

An absorption feature at or very close to 1.66 μm was found in fresh leaf spectra of manzanita and sumac (see Fig. 10 and Table 6). As observed for dried leaves of sagebrush and conifers, the fresh

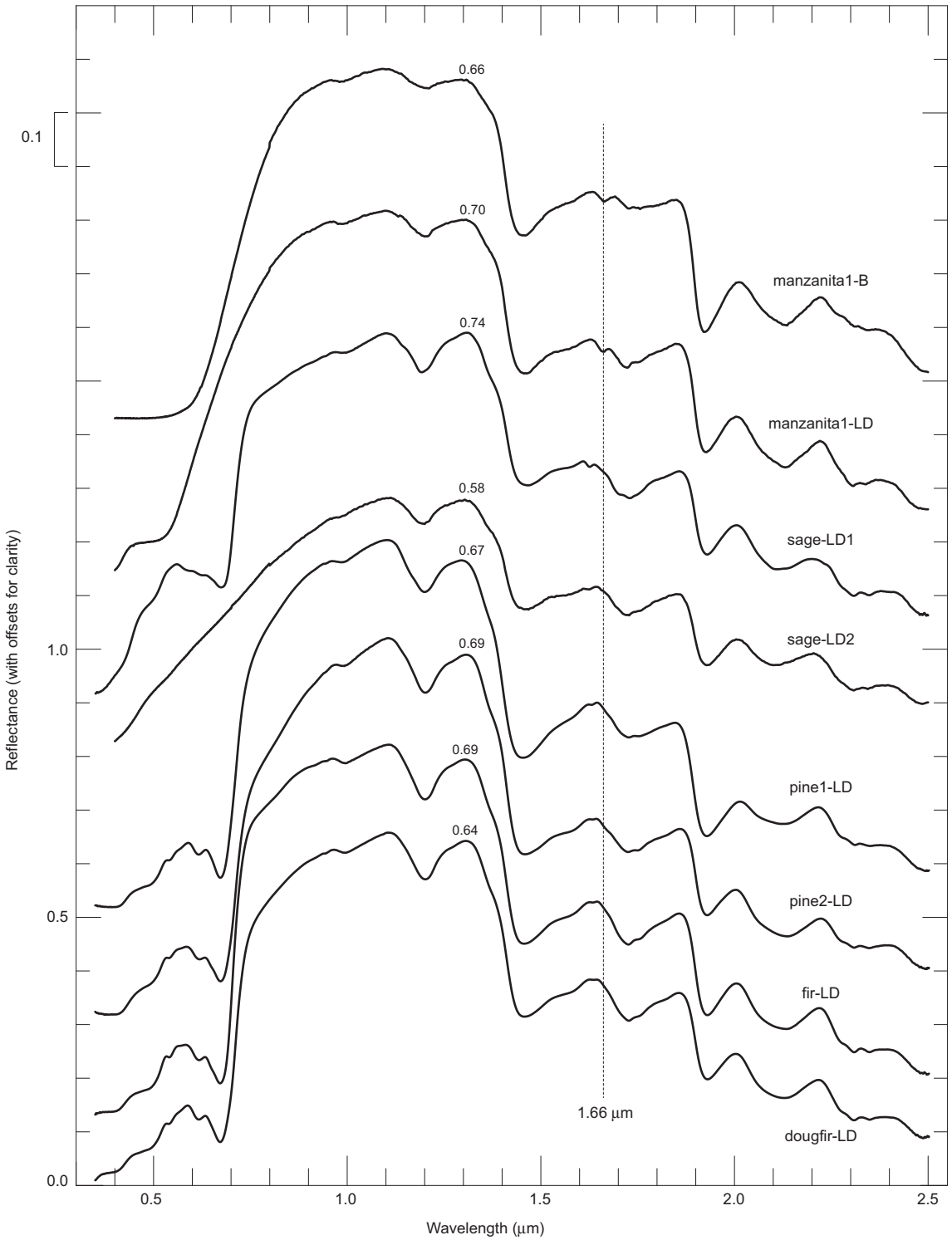


**Fig. 9.** Reflectance spectra of dried plant matter (see Table 2 for sample descriptions). Spectra are offset for clarity. From bottom to top spectrum, the offset values added to spectra are 0.0, 0.1, 0.3, 0.5, 0.7, 0.85, 1.1, and 1.4. The original reflectance values for channels at 1.3 μm are labeled next to each spectrum.

leaf spectra also show absorption features at shorter wavelength position. The feature in that sample of fresh sagebrush leaves is centered at 1.629 μm, close to the 1.625 μm feature in the spectra of dried sagebrush leaves. The spectra of fresh conifer needles had very weak features centered in the 1.632 to 1.636 μm region, as did the dried needles.

*Spectra of plants*

The spectra of whole plants show the same features (Fig. 11) and trends in feature positions (Table 6) as spectra of dried plant matter and fresh leaves. Manzanita, sumac and chokecherry have absorption features near 1.66 μm; feature centers are all within

**Table 6**
Feature parameters for absorptions near 1.66 μm in dry and fresh leaves, and plant canopies.

| | Plant material | Center (μm) | Depth | Width (nm) | Area (nm) |
|---|---|---|---|---|---|
| Leaves, dry | Manzanita1-B | 1.6629 | 0.0309 | 25.6 | 0.801 |
| | Manzanita1-LD | 1.6576 | 0.0250 | 20.0 | 0.513 |
| | Sage-LD1 | 1.6246 | 0.0139 | 13.5 | 0.189 |
| | Sage-LD2 | 1.6250 | 0.0074 | 16.1 | 0.117 |
| | Pine1-LD | 1.6331 | 0.0050 | 10.7 | 0.054 |
| | Pine2-LD | 1.6347 | 0.0021 | 8.9 | 0.018 |
| | Fir-LD | 1.6354 | 0.0024 | 9.6 | 0.023 |
| | Dougfir-LD | 1.6363 | 0.0011 | 9.2 | 0.010 |
| Leaves, fresh | Manzanita1-LF | 1.6572 | 0.0126 | 17.3 | 0.248 |
| | Manzanita2-LF | 1.6617 | 0.0184 | 18.5 | 0.342 |
| | Sumac-LF | 1.6559 | 0.0161 | 18.2 | 0.299 |
| | Sage-LF | 1.6289 | 0.0093 | 13.9 | 0.130 |
| | Pine1-LF | 1.6323 | 0.0025 | 10.0 | 0.025 |
| | Pine2-LF | 1.6339 | 0.0014 | 7.5 | 0.010 |
| | Fir-LF | 1.6358 | 0.0012 | 7.8 | 0.009 |
| Plants | Manzanita2-P1 | 1.6602 | 0.0148 | 17.1 | 0.254 |
| | Manzanita2-P2 | 1.6616 | 0.0151 | 16.8 | 0.260 |
| | Manzanita2-P3 | 1.6610 | 0.0144 | 17.3 | 0.249 |
| | Manzanita2-P4 | 1.6607 | 0.0096 | 18.8 | 0.177 |
| | Manzanita2-P5 | 1.6610 | 0.0164 | 17.1 | 0.287 |
| | Manzanita2-P6 | 1.6597 | 0.0127 | 18.1 | 0.227 |
| | Sumac-P | 1.6591 | 0.0045 | 14.7 | 0.067 |
| | Chokecherry-P | 1.6652 | 0.0014 | 8.8 | 0.014 |
| | Sage-P1 | 1.6302 | 0.0042 | 12.4 | 0.053 |
| | Sage-P2 | 1.6303 | 0.0022 | 12.9 | 0.029 |
| | Juniper-P | 1.6335 | 0.0086 | 13.3 | 0.116 |
| | Pine3-P | 1.6332 | 0.0020 | 10.1 | 0.020 |
| Tea (averaged parameters) | Dried leaves ($n = 56$) | 1.6629 | 0.0065 | 16.2 | 0.114 |
| | Fresh leaves ($n = 56$) | 1.6615 | 0.0014 | 7.6 | 0.015 |
| | Plant canopies ($n = 14$) | 1.6610 | 0.0021 | 8.7 | 0.022 |

5 nm of this position. The sagebrush plants have absorption features centered near 1.630 μm. The juniper and pine plants have weak absorption features centered near 1.633 μm.

*Spectra of tea with varying phenolic concentrations*

Phenolic concentrations in the dried tea leaves ranged from 14.7% to 29.5% by dry weight, with an average concentration of 19.3% (std. dev. = 4.6%). An absorption feature centered near 1.66 μm was found in all the spectra of dried, powdered leaves and fresh leaves (Fig. 12). On average, the absorption feature was most apparent in the dried leaves compared to the fresh leaves, as evidenced by greater average depths for dried leaves (Table 6). An absorption feature centered near 1.66 μm was found in only 13 of the 46 reflectance spectra of tea plant canopies using the fixed continuum endpoints. The automated SFA, with the adjustment of continuum endpoints, found an additional spectrum with an absorption feature, resulting in 14 spectra with the 1.66 μm absorption feature. Table 6 shows the average feature parameters for these 14 spectra. The 1.66 μm feature in canopy spectra is weaker compared to dry leaf spectra but stronger compared to fresh leaf spectra.

*Continuum-removed spectra for the 1.66 μm feature*

Continuum-removed spectra of the 1.66 μm feature in selected phenolic compounds, dried plant matter, fresh leaves and plants are shown in Fig.13a–e. The spectra have been scaled to equivalent depth so the shifts in feature center and spectral shape can be more clearly seen. Continuum-removed spectra of selected phenolic compounds are shown in Fig. 13a. On average, the lignin absorption feature is shifted 17 nm long ward of the tannic acid absorption feature. The lignin feature has the least overlap with the other phenolics shown in Fig.13a (gallic, ellagic, and tannic acids).

Fig. 13b shows the continuum-removed spectral features for selected samples from the ACCP data set. This figure illustrates the shift in wavelength position that was observed in the average feature positions for species (see Table 5). Red maple has an absorption feature at the shortest wavelength position. The feature in red spruce is centered at a longer wavelength position.

Positions of spectral features near 1.66 μm for different plant types are consistent across water status (dry vs. fresh) and measurement level (leaf vs. plant canopy), see Fig. 13c–e. Sagebrush has a feature at the shortest wavelength position, followed by pine and fir. Manzanita and sumac maintain absorption feature positions closest to 1.66 μm. These positions align most closely with the smaller phenolic compounds (gallic, ellagic, and tannic acid), which are short ward of the lignin absorption feature position.

*Tea phenolic concentrations and the 1.66 μm feature*

The absorption feature stays at a consistent position in the spectra of tea leaves and plants measured in both the dry and fresh states (Fig. 14a–c), varying approximately 2 nm from dry leaves to plant canopies (see Table 6). Linear regression results for the phenolic concentrations related to feature depths, widths and areas are shown in Table 7. Results are shown for parameter values derived from both fixed and adjusted continuum endpoints. At the dried leaf level, feature depths and areas had higher $r^2$ values than widths. The highest coefficient of determination and lowest RMSE values were obtained for the feature depths derived with fixed endpoints ($r^2 = 0.95$, RMSE = 1.0% phenol by dry weight). In contrast, the most accurate regression result for fresh leaves was obtained for feature areas derived from the adjusted continuum endpoints ($r^2 = 0.79$, RMSE = 2.1% phenol by dry weight). At the plant canopy level, regression results for spectra with the 1.66 μm feature were most accurate for feature areas derived using fixed continuum endpoints ($r^2 = 0.78$, RMSE = 1.0% phenol by dry weight). The scatter plots of the best regression results at each measurement level are shown in Fig. 15. Relative to the mean concentrations of phenols, the results were very good at the dried leaf and plant canopy levels, rRMSE of 4.8% and 5.1%, respectively. At the fresh leaf level, the rRMSE was lower, at 10.0%.

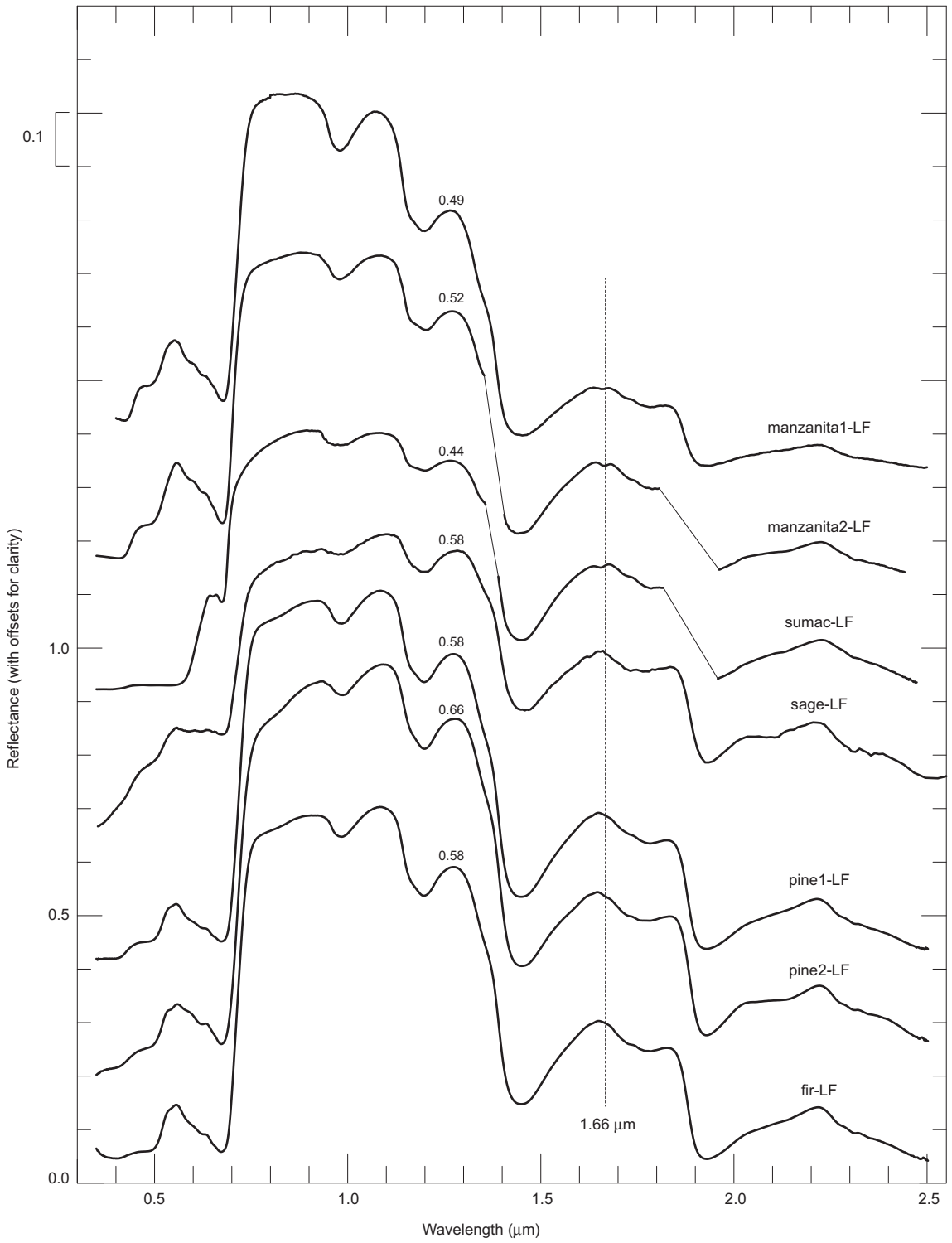


**Fig. 10.** Reflectance spectra of fresh leaves (see Table 2 for sample descriptions). Spectra are offset for clarity. From bottom to top spectrum, the offset values added to spectra are 0.0, 0.2, 0.4, 0.6, 0.9, 1.1, and 1.3. Channels in wavelength regions of strong atmospheric contamination have been removed and replaced with a thin line. The original reflectance values for channels at 1.3 μm are labeled next to each spectrum.

## Discussion

### *The 1.66 μm feature in phenolic compounds, dry leaf, fresh leaf and canopy spectra*

The spectra of the phenolic biochemical compounds have absorption features near 1.66 and 2.14 μm (see Fig. 6). These phenolic compounds differ in size and the types of substituent groups attached to the phenolic ring. Still, they share the commonality of at least one arene group (benzene ring) in their chemical structures. An absorption feature near the 1.66 μm position is also identifiable in spectra of plants measured at dry leaf, fresh leaf and canopy levels (see Figs. 8–12). For dry leaves, the feature is strongest in red maple, sugar maple, sumac, manzanita, and tea,

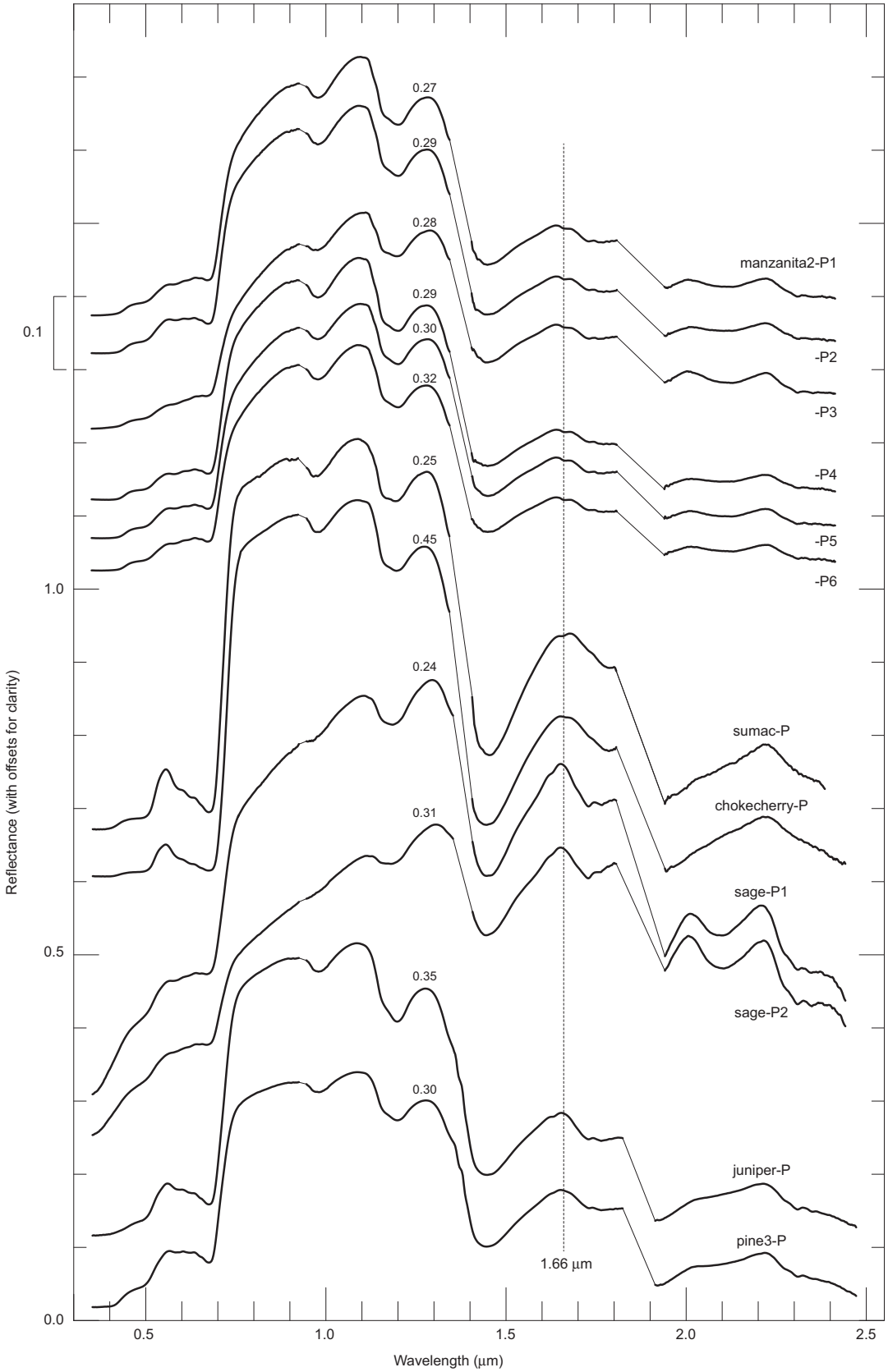


**Fig. 11.** Reflectance spectra of plant canopies (see Table 2 for sample descriptions). Spectra are offset for clarity. From bottom to top spectrum, the offset values added to spectra are 0.0, 0.1, 0.2, 0.25, 0.6, 0.65, 1.0, 1.05, 1.1, 1.2, 1.3 and 1.35. Channels in wavelength regions of strong atmospheric contamination have been removed and replaced with a thin line. The sagebrush spectra were scaled by a multiplicative factor of 2.0 before the offset was added. The original reflectance values for channels at 1.3 μm are labeled next to each spectrum.

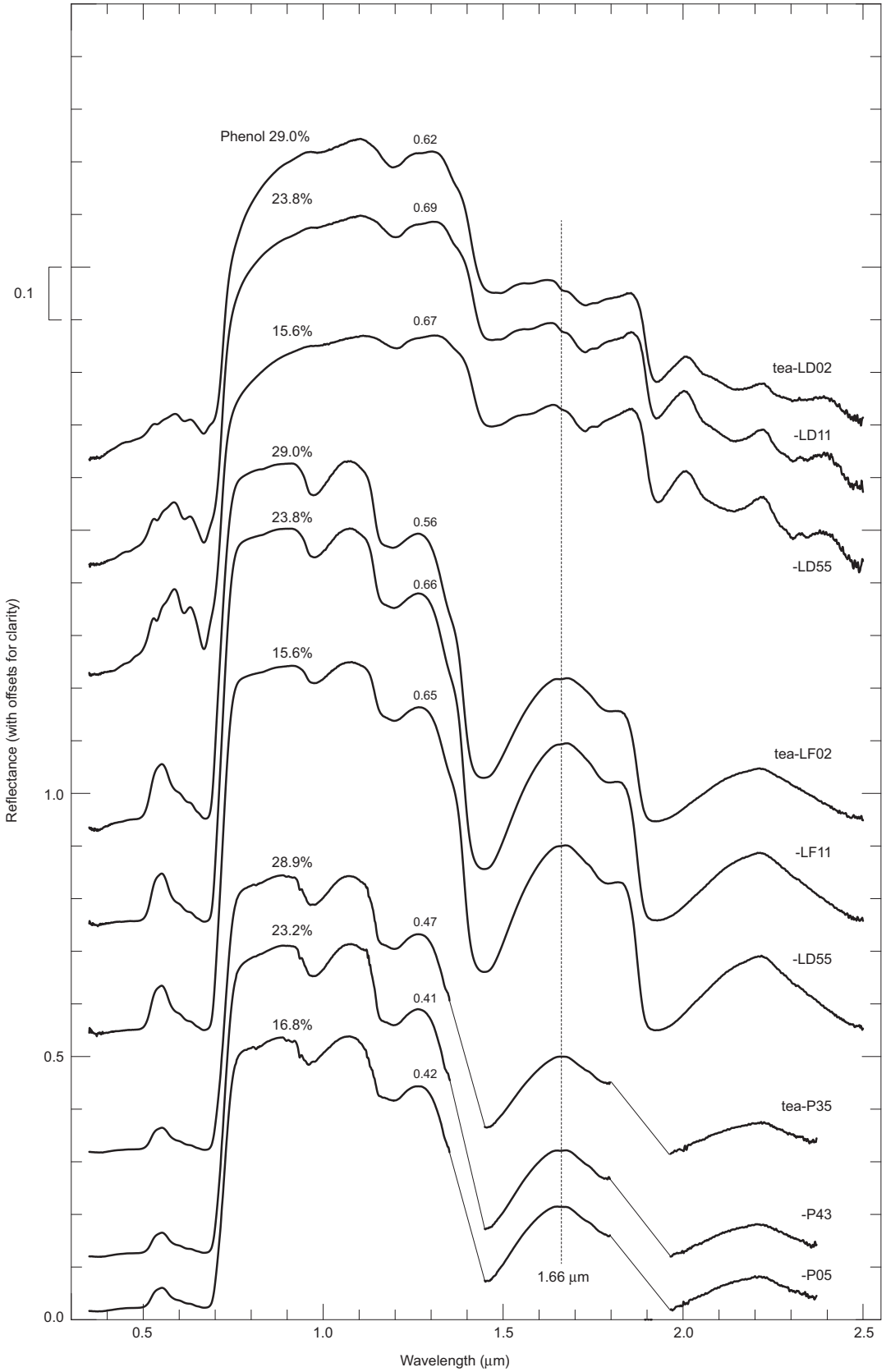


**Fig. 12.** Reflectance spectra of tea, including dried, ground leaves (-LD), fresh leaves (-LF), and plant canopies (-P). Spectra are offset for clarity. From bottom to top spectrum, the offset values added to spectra are 0.0, 0.1, 0.3, 0.5, 0.6, 0.9, 1.2, 1.4, and 1.6. Channels in wavelength regions of strong atmospheric contamination have been removed and replaced with a thin line. The original reflectance values for channels at 1.3 μm are labeled next to each spectrum.

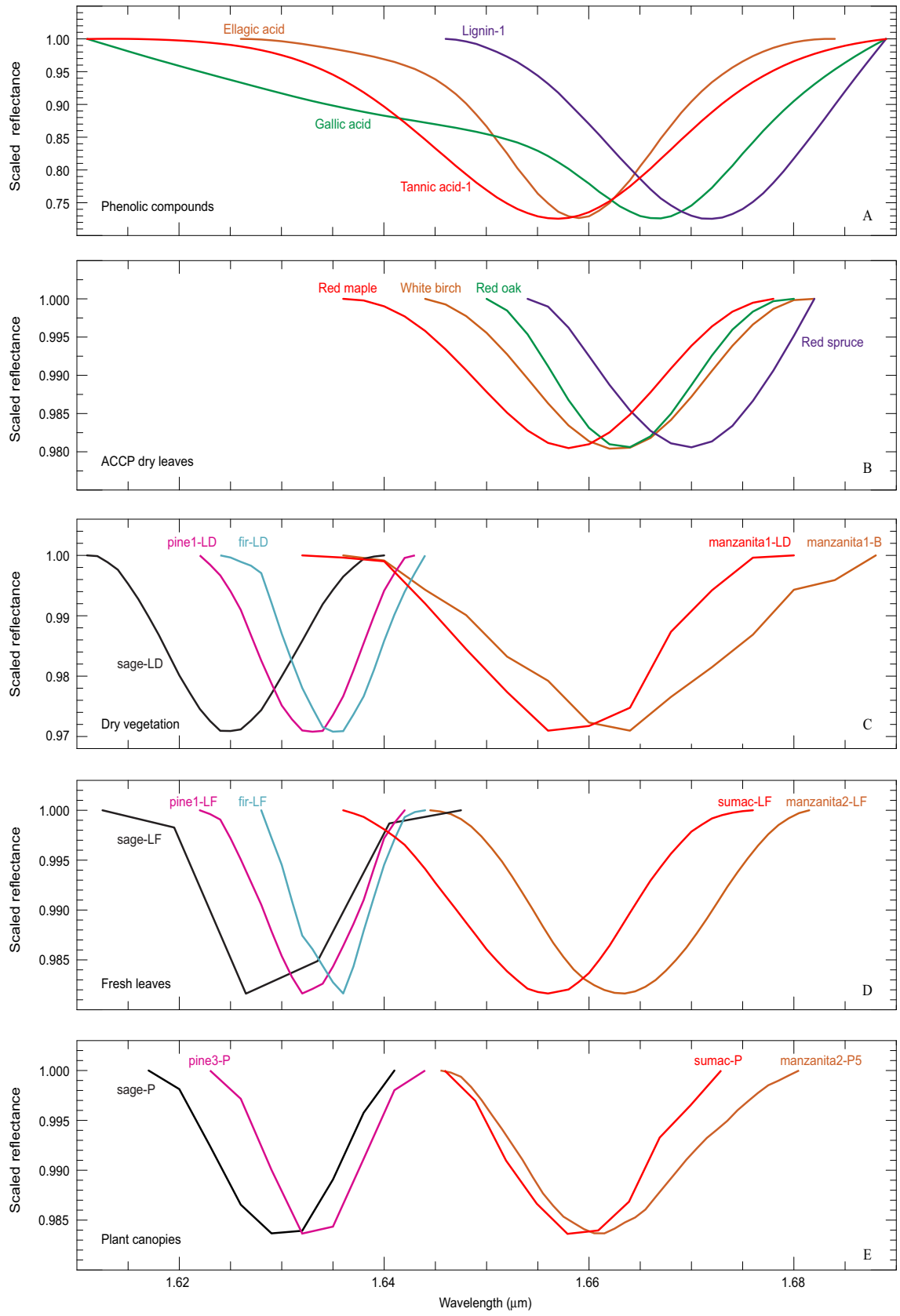


**Fig. 13.** Continuum-removed spectra for features near 1.66 μm: (A) phenolic compounds; (B) ACCP dry leaf samples; (C) dried leaves; (D) fresh leaves; and (E) plant canopies. Features have been scaled to equivalent depth in each panel.

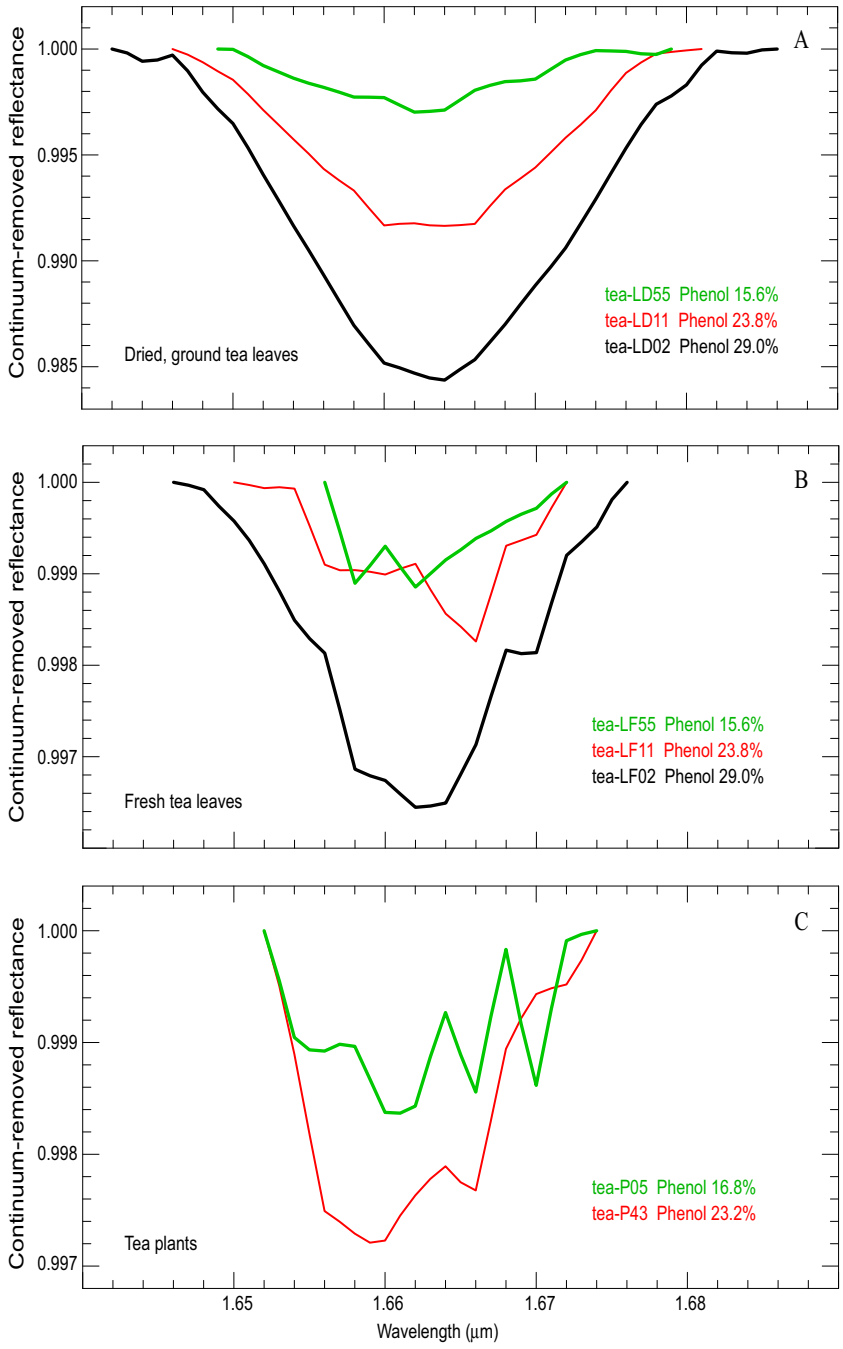


**Fig. 14.** Continuum-removed features near 1.66 μm in tea spectra: (A) dried, ground leaves; (B) ACCP fresh leaf samples; and (C) plant canopies. Features have been scaled to equivalent depth.

but is also present in white birch, red oak, and white oak. Elvidge (1990) noted that "absorptions at 1.66 and 2.13 μm suggestive of tannin were observed in several dry plant material spectra." In the spectra of phenolic compounds, these features are both present. However, in the spectra of plant matter presented in this paper, we see more clearly and consistently the 1.66 μm feature across a variety of species and phenolic compounds.

The 2.14 μm feature is much broader than the narrow 1.66 μm feature and overlaps more with other major plant constituents than the 1.66 μm feature (see Fig. 7). In comparison to the fine structure seen in the 2.0–.5 μm region of spectra of ellagic acid and the smaller phenolics, tannic acid is more smoothly varying with a broad absorption feature centered at 2.137 μm (see Fig. 6). This change could be caused be a function of the larger size of the tannic acid molecule and/or the absorption by the non-phenol portions of the tannic acid. Tannic acid composition depends on the source material, typically, tara pods (*Caesalpinia spinosa*), gallnuts from *Rhus semialata* or *Quercus infectoria,* or Sicilian sumac leaves (*Rhus coriaria*). But commercial tannic acid is often described as decagalloyl glucose ($C_{76}H_{52}O_{46}$; see the chemical structure in Fig. 1). Glucose has a broad absorption feature centered at 2.111 μm (Fig. 16; D-(+) glucose purchased from Sigma–Aldrich #G8270). Thus, it is likely that the 2.1 μm region of tannin and lignin spectra are influenced by their glucose components.

In comparison to the 2.14 μm feature, the absorption at 1.66 μm is at a unique position compared to the major plant biochemical constituents: cellulose, starch, and protein, which also have reflectance peaks near this wavelength (see Fig.7). Absorption fea-

**Table 7**
Linear regression results for parameters of the 1.66 μm absorption feature and phenolic concentrations in tea.

| Tea mesurement level | *n* | Continuum endpoints | Feature parameter | Regression results $r^2$ | RMSE (%phenol) | Relative RMSE (%) (RMSE/sample mean) × 100 | *F* |
|---|---|---|---|---|---|---|---|
| Dried and ground leaves | 56 | Fixed | **Depth** | **0.95** | **1.0** | **4.8** | **1098** |
| | | | Width | 0.72 | 2.4 | 11.7 | 137 |
| | | | Area | 0.95 | 1.0 | 4.9 | 1042 |
| | 56 | Adjusted | Depth | 0.94 | 1.1 | 5.5 | 805 |
| | | | Width | 0.87 | 1.6 | 7.8 | 369 |
| | | | Area | 0.92 | 1.3 | 6.1 | 638 |
| Fresh leaves | 56 | Fixed | Depth | 0.45 | 3.4 | 16.3 | 44 |
| | | | Width | 0.56 | 3.0 | 14.6 | 68 |
| | | | Area | 0.57 | 3.0 | 14.3 | 73 |
| | 56 | Adjusted | Depth | 0.73 | 2.4 | 11.4 | 146 |
| | | | Width | 0.64 | 2.7 | 13.2 | 95 |
| | | | **Area** | **0.79** | **2.1** | **10.0** | **208** |
| Plant canopies | 13 of 46 total | Fixed | Depth | 0.75 | 1.1 | 5.5 | 33 |
| | | | Width | 0.73 | 1.2 | 5.8 | 29 |
| | | | **Area** | **0.78** | **1.0** | **5.1** | **40** |
| | 14 of 46 total | Adjusted | Depth | 0.63 | 1.4 | 6.7 | 21 |
| | | | Width | 0.46 | 1.6 | 8.2 | 10 |
| | | | Area | 0.63 | 1.4 | 6.7 | 21 |

Boldface indicates the most accuracte result for each measurement level.

tures in the glucose spectrum (see Fig. 16) do not align with tannic acid and lignin in the 1.66 μm region. These characteristics suggest that the 1.66 μm feature has greater potential compared to the 2.14 μm feature as a direct indicator of the presence of phenolic compounds. Furthermore, tannic acid and the smaller phenolics have features slightly short ward of the lignin absorption feature at 1.67 μm (see Table 4 and Figs. 7 and 13a), indicating some possibility that the wavelength position of the absorption feature could be used to distinguish tannic acid and other small phenolic molecules from the larger lignin molecules. While, the 2.14 μm region is affected by phenolic compounds, the overlapping absorptions by other plant constituents make it more complicated to detect phenolic compounds uniquely. For these reasons, we focused on the 1.66 μm feature; however, follow-on studies of the influence of phenolics on the 2.0–2.2 μm region are warranted.

At the fresh leaf level, our perception of the expressions of plant biochemistry on reflectance spectra has been hindered by the overlapping absorptions by water (Gao and Goetz, 1994, 1995; Ramoelo et al., 2011). In this study, the 1.66 μm feature absorption feature remains evident in both dried and fresh leaves of certain species. The feature persists in manzanita at the dry leaf, fresh leaf, and plant canopy levels of measurement (see Figs. 9–11 and 13c–e). The 1.66 μm absorption feature is consistent in spectra of dried and fresh leaves of tea. For tea canopies, the feature is only evident in one-third of the spectra. Overall, the depth of the feature lessens from the dry leaf to the whole plant level (see Table 6 and Fig. 14). At the leaf level, the likely cause of the weakening is water. Water has an absorption feature centered near 1.445 μm (Kokaly et al., 2009) that extends into the 1.66 μm region. This water absorption lowers the short wavelength shoulder of the 1.66 μm absorption feature and, thus, lessens the depth of the continuum-removed feature. At the canopy level, the weakening of the feature is also consistent with integration of shadow and background materials into the reflectance measurement.

Despite the effect of water and other influences at the canopy level, the feature near 1.66 μm can be seen in vegetation spectra presented in past reflectance and remote sensing studies. Roberts et al. (2004) present spectra of conifer bark with a feature near this position (for western hemlock, *Tsuga heterophylla,* and Douglas-fir, *Pseudotsuga menziesii*). In that study, the branch scale spectra of *Populus trichocarpa* and Pacific silver fir (*Abies amabilis*) also appear to have a weak feature near 1.66 μm. In Schaepman et al. (2009), fresh leaf spectra of three dominant species from the Elburz Mountains, Iran, have an absorption feature near 1.66 μm (European hornbeam, *Carpinus betulus*; oriental beech, *Fagus orientalis*; and chestnut-leaved oak, *Quercus castaneifolia*).

Without chemical determination of the phenolic subclasses in our samples, we cannot confirm exactly which phenolic substances contribute to the 1.66 μm absorption. However, given the diversity of species in which the 1.66 μm feature was observed in this study and the references to other studies, it is reasonable to hypothesize that a variety of plant phenolics give rise to this absorption in vivo. In addition to linking the feature to phenolics in tea, we document this feature occurring clearly in spectra of other plants, including: sumac (*Rhus* sp.), maple (*Acer* sp.), birch (*Betula* sp.), manzanita (*Arctostaphylos* sp.), and chokecherry (*Prunus* sp.). Many of these species have been studied for their relatively high concentrations of various phenolics. *Rhus* species have elevated levels of gallic acid based tannins (Haslam, 2007) and are among the classic sources for tannic acid, of the hydrolysable tannin class. *Acer* species have also been the subject of study for phenolics and variation in tannin chemistry (Bate-Smith, 1977; Haslam, 1965). Baldwin et al. (1987) reported phenolic levels up to 20% by dry weight in *A. saccharum*. They also observed phenolic concentrations of more than 10% in *Betula allegheniensis*. Shure et al. (1998) tracked total phenolic and hydrolysable and condensed tannins in oak forests through three years and showed high levels of these substances in *A. rubrum* and *Q. alba*. Oak species are well known for the tannins in their leaves, bark, and galls, which were historical resources for extracts to tan leather hides and to use in medicinals (Paaver et al., 2010; Haslam, 1989; Déyeux, 1793). Several species of oaks (*Q. robur* L. and *Q. rubra*) have been studied with respect to the impact of moth larvae on phenolic concentrations (Schultz and Baldwin, 1982; Feeny, 1970). *Arctostaphylos glauca* and *A. glandulosa* contain several phenolic compounds which were, for a time, attributed to allelopathy in California chaparral ecosystems (Chou and Muller, 1972; Muller et al., 1968). Some species of *Prunus* are known to produce proanthocyanidins (Haslam, 2007; Bryant et al., 1987).

### *Estimating plant phenolic concentrations using reflectance spectra*

The distinct position of the absorption feature at 1.66 μm compared to the absorptions of lignin, cellulose, and other major plant biochemical components suggest the detection and quantification of plant phenolics using reflectance spectra could be robust. The unique positioning of absorption features has been shown to be

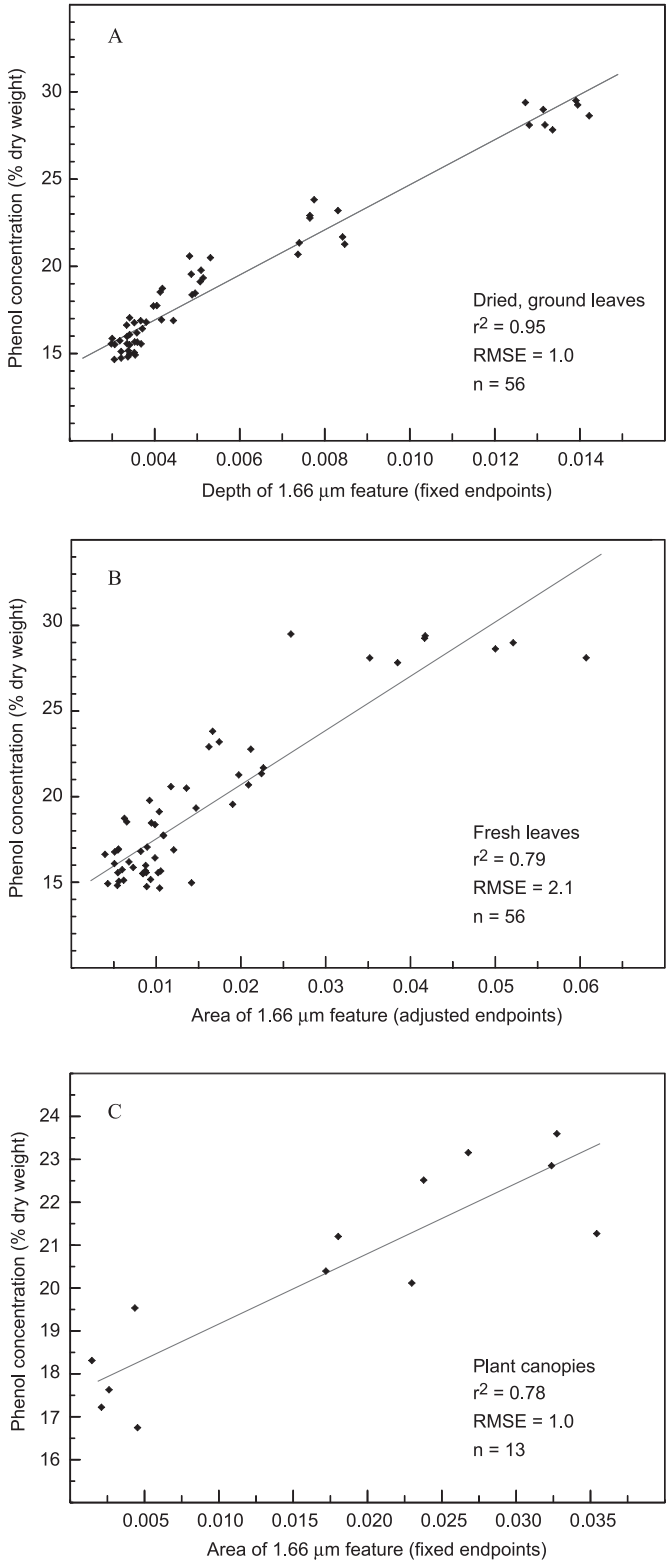


**Fig. 15.** Linear regression results for 1.66 μm feature parameters and tea phenolic concentrations: (A) feature depths with fixed endpoints for dried, ground leaves; (B) feature areas with adjusted endpoints for fresh leaves; and (C) feature areas with fixed endpoints for plant canopies.

a strong underpinning for statistical methods that utilize spectra to quantify plant biochemistry. Kokaly (2001) showed the positions of protein absorption features at 2.05–2.17 μm were offset compared to the cellulose and lignin absorption features centered near 2.10 μm. The unique positioning of these features, caused by N-containing amide bonds, contributes to the successful quantification of leaf N from reflectance spectra even though it is far less abundant than cellulose and lignin. Leaf N is typically less than 4% by dry weight. Together, lignin and cellulose are usually greater than 60% of the weight of dried leaves (Kokaly and Clark, 1999).

The persistence of the 1.66 μm absorption feature in fresh leaf and plant spectra gives strong support to past studies that have used reflectance spectra to predict concentrations of phenolics. Windham et al. (1988) found that the wavelength 1.664 μm was of the highest importance in predicting tannin concentrations using the reflectance spectra of dried and ground leaves of the legume *Sericea lespedeza*. Ferwerda et al. (2006), in relating first derivatives of reflectance of fresh and senescent mopane (*Colophospermum mopane*) leaves to tannin content, found that wavelength 1.640 μm was selected during bootstrap phase, though it was not used in the final prediction model. Bian et al. (2010) predicted tea polyphenol concentrations using PLSR, again using first derivative of reflectance. That study showed good results for both dried and fresh leaves and high correlations in the 1.66 μm region. Bian et al. (2013) extended this work to field spectra of plant canopies with good success, but did not find that data in the 1.66 μm region played an important role in predicting tea polyphenols at the canopy level.

While such statistical studies are of great utility in an applied way, they use methods that utilize all channels in a spectrometer to generate correlations, a strength in developing relationships for specific sample populations. However, these methods do not focus on specific wavelengths where the biochemical of interest has its greatest effect. Past studies have shown that direct focus on absorption feature parameters can result in high correlations with plant chemistry (Kokaly and Clark, 1999; Kokaly, 2011; Girma et al., 2013; Malenovský et al., 2013) and detection of stress (Sanches et al., 2014). In this study, we directly related the 1.66 μm absorption feature parameters (depth, width, and area) to phenolic concentrations for the tea spectra of Bian et al. (2013) using simple linear regression (see Table 7). At the dry leaf level of measurement, very strong relationships were found with feature depth and area and phenolic concentrations using both fixed and adjusted continuum endpoints ($r^2 \geq 0.9$ and RMSE $\leq 1.3$). These results are comparable, though not quite as high, as those obtained by Bian et al. (2010, 2013),) using PLSR.

At the fresh leaf level, the coefficients of determination were lower and the RMSEs were higher than the dry leaf results (see Table 7). Possible reasons for the weaker relationships are: (1) the impact of leaf water, and (2) the lower signal:noise ratio (SNR) of the fresh leaf measurements. The fresh leaves were measured in thick stacks which accentuates the absorption by leaf water for radiation that penetrates each leaf layer. As discussed, leaf water lessens the apparent strength of the 1.66 μm feature. As the number of layers increases, water absorption dominates stacks of fresh leaves and reduces the features of other plant constituents. As noted earlier, depths of the 1.66 μm feature were greater in canopy spectra than fresh leaves. If the leaves were stacked in piles higher than the canopy leaf area index, the water absorption in the fresh leaf measurement will be greater than the canopy and the fresh leaf 1.66 μm feature depth reduced compared to the canopy.

Measurement SNR greatly impacts fresh leaf spectra because reflectance (signal) is low due to water and the 1.66 μm feature is weakened by water. Thus, noise is more evident in the continuum-removed spectra of fresh leaves (compare Fig. 14a and b). Future studies should increase the integration times for dark current, white reference, and sample spectra, and increase the number

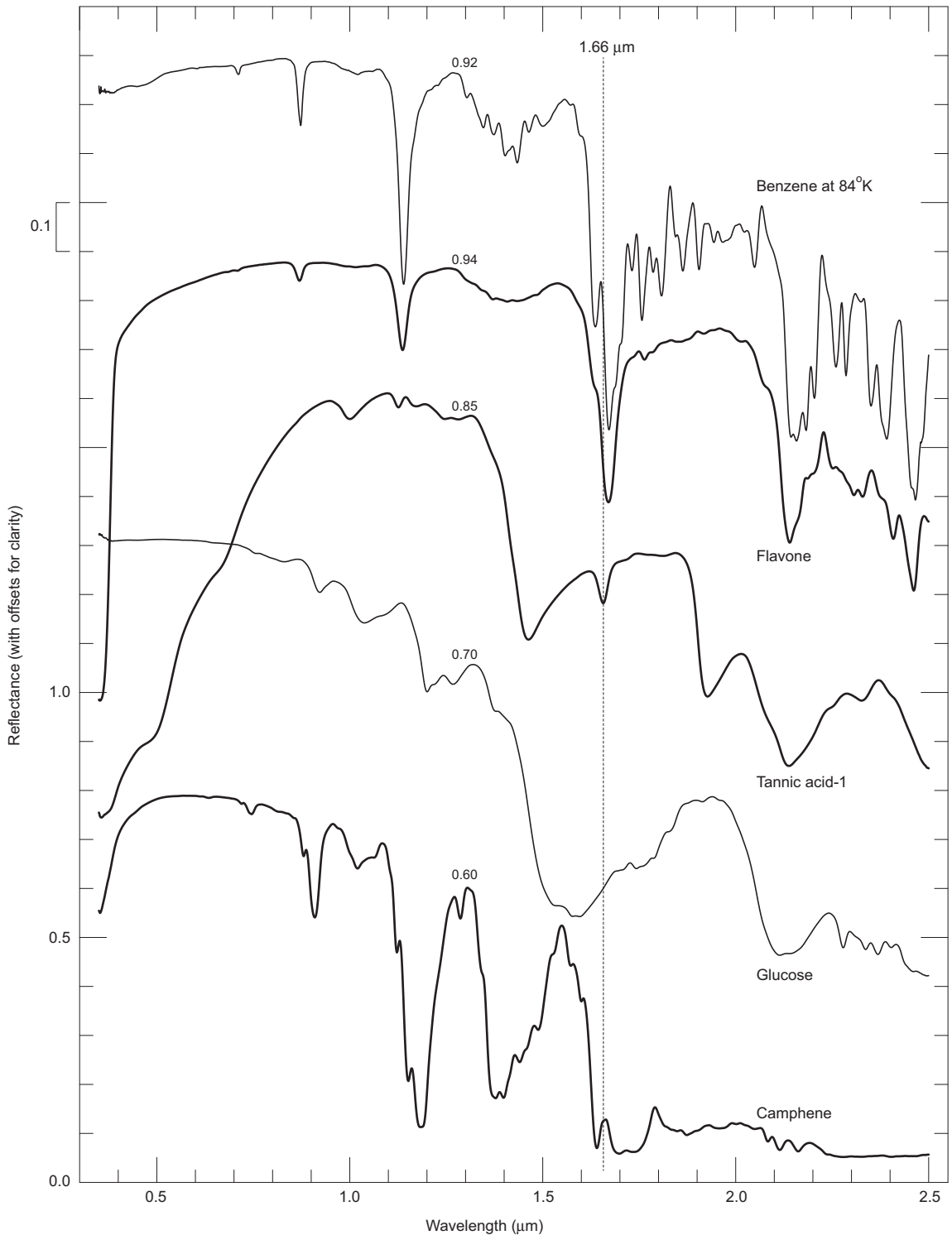


**Fig. 16.** Reflectance spectra of camphene, glucose, tannic acid, flavone, and benzene. Spectra are offset for clarity. From bottom to top spectrum, the offset values added to spectra are 0.0, 0.35, 0.6, 0.9, and 1.3. The original reflectance values for channels at 1.3 μm are labeled next to each spectrum.

of spectra recorded so that the SNR of the average spectra are increased.

At the canopy level, the impact of low SNR may help to explain why only 14 of 48 spectra showed evidence of an absorption feature at 1.66 μm. In addition to leaf water effects, canopy shadows further decrease reflectance levels and lower SNR (see Figs. 12 and 14). Despite these effects at the canopy level, good correlations were still found between phenolic concentrations and feature parameters derived using fixed continuum endpoints (see Table 7). The best correlation was found with feature area ($r^2$ = 0.78, RMSE = 1.0% phenol by dry weight, rRMSE = 5.1%, $n$ = 13). Bian et al. (2013) used PLSR and achieved high correlations at canopy level ($r^2$ = 0.84, RMSE = 1.4% phenol by dry weight, rRMSE = 6.8%, $n$ = 48). However, they found that wavelengths in the 1.66 μm region did not have an important role in predicting tea polyphenol concentrations, possibly indicating that the influences of other plant biochemical constituents were driving the high correlations achieved by PLSR, as suggested by Bian et al. (2013).

An important consideration in applying reflectance spectra to predict plant composition is the accuracy of any wet chemistry method used to determine biochemical concentrations. The most common chemical method for determining phenolic content is the Folin-Ciocalteu Reaction (FCR; Folin and Ciocalteu, 1927). FCR was initially developed for protein analysis through the reagent's activity toward protein tyrosine residues. It was later utilized by Singleton and Rossi (1965) to quantify total phenols in wines. However, Singleton et al. (1999) noted the many potential interfering substances which can inhibit, add, or enhance the color change in the reagent, including aromatic amines, aminophenols, indoles, purines, proteins, sugars, ascorbate, citrate, and sulfite. Huang et al. (2005) suggest that a more descriptive term for FCR is as a measure of "reducing capacity" rather than "total phenolic capacity." The various phenolic compounds have differing degrees of activity in FCR. These issues with FCR has led some researchers to use other approaches, such as enzymatic methods, for quantifying total phenolic content in tea and wine (Stevanato et al., 2004). Because of the variable reaction of phenolic compounds to the reagent and the interferences from other substances, FCR results obtained for one sample type are not necessarily comparable to other samples types. The chemical nature of FCR is still undefined, but it is convenient and simple. Still, comparison of FCR results between species should be done with careful consideration of plant phenolic composition and potential interference between phenolic compounds.

*Identifying the chemical bonds contributing to the 1.66 μm absorption feature*

Given the consistency of the 1.66 μm absorption feature in plant phenolics, its identification in leaf and plant spectra, and its usefulness in quantifying the phenolic concentrations in vegetation, several questions are provoked: (1) what is the specific chemical bond that causes the absorption, (2) is that bond common in other biochemical constituents of plants, and (3) how is it affected by molecule size and neighboring bonds (i.e., how much does the feature shift in wavelength position and feature shape from gallic acid to tannic acid to lignin). Development of this knowledge is needed generally to improve our understanding of plant reflectance and could be used for separating the influences of small phenolics on reflectance spectra as distinct from lignin.

Windham (1988) suggested the 1.664 μm region was influenced by the first overtone of a C—H stretching fundamental in the aromatic portions of tannins, citing (Wheeler, 1959). Cloutis (1989) in a study of hydrocarbons, reports the first overtone of the aromatic C—H bond to be in the region of 1.65 μm. Fig. 16 shows that spectrum of benzene, measured frozen at 84 degree K (Clark et al., 2010), has an absorption feature centered at 1.672 μm. At this wavelength, there is also a peak in the spectrum of the absorption coefficient of liquid benzene at room temperature (spectrum not shown here). Flavone, the non-hydroxylated baseline molecule to the flavonol phenolic class (such as quercetin), has a strong absorption feature at 1.67 μm. These molecules differ from phenolics by the absence of hydroxyl (—OH) in their chemical structure; but they still have absorption at a similar position. This is consistent with an interpretation of the 1.66 μm feature in plant spectra as arising from the first overtone of the C—H bond in carbon atoms on the aromatic rings in phenols (aromatic methine functional group —CH) and not the hydroxyl group bound to the aromatic rings in these molecules (Barton and Himmelsbach, 1993). This means that the physical basis for linking phenolic concentrations and reflectance variations in the 1.66 μm region is absorption by a functional group that is not limited to just phenols. Non-hydroxylated aromatic rings can and do exist in other plant biochemical components (e.g., in amino acids like phenylalanine). Thus, this study does not attribute the 1.66 μm feature solely as a phenolic absorption. Likely, the 1.66 μm feature is indicative of plant aromatics as a general class. Though, such casual attributions should not be made without more comprehensive studies on the in vivo chemical state of phenolic, non-hydroxylated aromatics, and similar molecules, their relative abundances in plant matter, and their expression on leaf and plant reflectance.

*Distinguishing the spectral influences of tannin and smaller plant phenolics from lignin*

Conclusive separation of the spectral impacts of tannic acid and smaller phenolics from lignin requires a comprehensive database of spectra and biochemical concentrations and leaf reflectance, more comprehensive than we have studied in this paper. The tea spectra have associated phenolic concentrations but lack quantification of the major plant biochemical, including lignin, cellulose, and protein (or nitrogen as a proxy for protein). The ACCP dataset has good quantification of these major plant constituents, but lacks data on phenolics. However, since the 1.66 μm feature is expressed in some species which are expected to be enriched in tannins and other phenolics (e.g., red maple), we examined, to the extent possible, the shift in the 1.66 μm spectral feature across species in the ACCP data set.

First, we examined the spectra of samples with high lignin concentration in the ACCP data set. These samples had lignin concentrations greater than or equal to 30% by dry weight. We saw no evidence of an absorption feature at 1.66 μm in these spectra.

Second, we examined the shift in the 1.66 μm feature in relation to the major plant constituents, lignin and cellulose. In the ACCP data set, the feature is strongly and consistently evident in the spectra of all or most samples of red maple, sugar maple, and white birch. The absorption feature is slightly shifted to longer wavelengths in the spectra of a lesser fraction of samples of other species (red oak and white oak). In spectra of samples of white pine and red spruce the feature has shifted away from the 1.66 μm absorption and closer to the 1.67 μm position.

Both the abundance of phenolic components and the influence of non-phenolic biochemical constituents in plants could be influencing the shift in the feature from 1.66 to 1.67 μm. Lower concentrations of non-lignin phenolics could result in the absorption feature being positioned closer to 1.67 μm. On the other hand, higher concentrations of lignin in pine and spruce may be the cause of this shift. The ACCP data on lignin concentrations shows that in both absolute values and as a ratio to cellulose, lignin is more dominant in pine and spruce biochemistry compared to the maples and oaks (see Table 5). This suggests that the expression of the 1.66 μm absorption feature in plants could be reduced in appearance by the dominance of lignin in leaves.

Soukupová et al. (2002), in examining measured spectra of liquid phenolics and lignin and tannin powders, suggested that lignin concentrations calculated on the basis of near infrared spectral characteristics could be greatly influenced by other phenolic compounds such as tannins. They suggested that variations in phenolic content could be a reason why lignin prediction tends to have lesser performance than cellulose and nitrogen prediction in studies relating plant reflectance and biochemistry. We approach that issue in a different way in this study, seeing that for species with lower lignin concentration, the 1.66 μm feature related to phenolics is strongly expressed. For species with higher lignin concentration the feature is no longer directly detectable as a dip in the reflectance curve.

To improve reflectance based estimates of phenolics and lignin and to better understand shifts in absorption feature positions in plant spectra, a more comprehensive quantification of these compounds in leaf samples needs to be coupled with high quality spectral measurements. The quantification should include the subcomponents of larger phenolics, for example, condensed and

hydrolysable tannins and the monolignol subunits of lignin. From a broader perspective, we need to move from a gross oversimplification of plants as containing generic "dry matter" with three associated absorption regions in the SWIR (1.7, 2.1 and 2.3 μm) to a more detailed understanding of how the subtle expressions of specific chemical bonds in the large biochemical components of plants cause wavelength shifts and shape changes in the SWIR region. For example, the shifts and shape changes observed in the 2.1 and 2.3 μm features of plants as a function of lignin:cellulose ratio (Kokaly et al., 2007, 2009).

*Absorption features centered near 1.63 μm in sagebrush and evergreens*

Spectra of sagebrush leaves, evergreen needles, and plant canopies have an absorption feature near 1.63 μm feature (see Figs. 9–11 and 13 and Table 6). Given that the phenolic absorption feature centers are in the range of 1.653–1.672 μm, the absorption feature in these sage and evergreen plants is likely due to a different biochemical, perhaps a constituent of minor and/or highly variable concentration, as other spectra of these vegetation types were examined which did not exhibit a 1.63 μm feature. In other studies of sagebrush spectra (Mitchell et al., 2012), dry leaves of big sagebrush clearly show an absorption feature near 1.63 μm. The feature also appears to be weakly present in the canopy spectra of big sagebrush in that study.

*Artemisia* species can have elevated concentrations of terpenes and terpenoids, including acyclic molecules, such as artemisia ketone and myrcene, cyclic molecules, such as artemiseole and camphor, and bicyclic monoterpenes, such as α-pinene, camphene, and 1,8-cineole (Kelsey et al., 1983; Lopes-Lutz et al., 2008). Concentrations of these constituents can shift seasonally, with leaf age, and in response to herbivory (Kelsey et al., 1983; Lopes-Lutz et al., 2008). Terpenes are also prevalent in conifers in cyclic and acyclic forms, including enantiomers of α- and β-pinene, camphene, sabinene, terpinolene, and sesquiterpenes, such as humulene, caryophyllene, and longifolene (Pureswaran et al., 2004). It is possible that one or more classes of terpene could be causing the absorption near 1.63 μm. In contrast to phenolic compounds; terpenes do not have aromatic groups in their structure. Non-oxygenated, linear hydrocarbons tend to have absorption features closer to 1.7 μm (Kokaly et al., 2013), as has cineole (Wilson et al., 2001). But overtones of absorption by C—H have been seen to shift to shorter wavelengths when linked to terminal epoxide groups (Wheeler, 1959), suggesting that terpenes with such groups might be a possible cause of this absorption in sagebrush and evergreens.

Fig. 16 shows the spectrum of camphene, a bicyclic monoterpene. In addition to a broad absorption feature centered at 1.7 μm, camphene has a strong, narrow absorption feature centered at 1.639 μm. The 1.639 μm feature of this terpene is a closer match to the absorption features in conifer and sage than the phenolic absorptions near 1.66 μm. A small peak in the absorbance spectrum of eucalyptus oil (a steam distillate of eucalyptus leaves and terminal stems rich in the terpene 1,8-cineole) can be discerned in the 1.63–1.64 μm range in Wilson et al. (2001). If terpenes can be linked to the 1.63 μm feature, a possible explanation for the lack of consistency in the presence of the feature are the wide range in terpene concentrations within foliage of a single plant and between plants in the same area (Pureswaran et al., 2004). Additional research is warranted to more fully examine the terpene components of plants and the absorption features of pure terpene compounds in relation to the spectral features in dry and fresh leaves and plant canopies shown in this study.

*Phenolic constituents and ecological studies*

While the focus in this study has been on the spectroscopic aspects of plant phenolics, the development of such fundamental knowledge for quantifying them at leaf and canopy levels has potential benefits to ecological studies. Wilt and Miller (1992) investigated the seasonal variations in phenolic composition among different species and subspecies of sagebrush, including constituents that inhibit grazing herbivory. Skidmore et al. (2010) applied airborne imaging spectrometer data to reveal the spatial patterns of polyphenols and nitrogen in mopane trees and shrubs across a savanna landscape. Differences in polyphenol concentrations related to soil composition (affected by geologic parent material) and disturbance history (fire). From the ecosystem perspective of grazing wildlife, Skidmore et al. (2010) demonstrated the potential of canopy biochemical determinations from remote sensing for studying spatial patterns of both available resources and potential chemical inhibitors, by mapping N and polyphenol concentrations, respectively. Recent studies have focused on how the diversity in phenolics can be related to taxonomic classes in tropical forests. Asner et al. (2011) found wide ranges in phenolic concentrations (5–358 mg/g) in species from a lowland Borneo forest. The phenols and tannins were found to be important to separating canopy plants at the species, genus, and family levels (Asner et al., 2012).

## Conclusions

A weak, narrow absorption feature centered near 1.66 μm was detected in the spectra of dry leaves, fresh leaves, and plant canopies of several species. The feature was strongest and most persistent in spectra of manzanita, sumac, red maple, sugar maple, and tea. This feature appeared consistent with absorption caused by the first overtone of the aromatic C—H bond present in in phenolic compounds and non-hydroxylated aromatics. Lignin had an absorption feature shifted to slightly longer wavelengths (1.67 μm) compared to the smaller phenolic compounds, such as tannic acid, ellagic acid, gallic acid. Overlapping absorption by water was observed to cause apparent weakening of the 1.66 μm feature in fresh leaf and canopy spectra compared to dry leaf measurements. The weakening was evidenced by reduced feature depths, widths, and areas computed using continuum removal and spectral feature analysis methods.

Simple linear regressions of 1.66 μm feature depths, widths and areas with phenolic concentrations in tea resulted in high correlations and low errors at all measurement levels (dry leaf feature depth, $r^2 = 0.95$, RMSE = 1.0%, $n = 56$; fresh leaf feature area, $r^2 = 0.79$, RMSE = 2.1%, $n = 56$; and canopy feature area, $r^2 = 0.78$, RMSE = 1.0%, $n = 13$). The strengths of these relationships are comparable, though slightly lower, to past studies that used full spectra and PLSR statistical methods to predict phenolic concentrations. By contrast, in this study only a single, individual feature parameter derived directly from the 1.66 μm feature was used in each simple linear regression analysis.

The potential utility of weak spectral features underscores the need for robust practices in spectral measurements, including validation of sensor wavelength and bandpass performance, collection of measurements with high signal-to-noise ratio, and conversion of spectra to absolute reflectance. The degree to which the 1.66 μm absorption feature can be directly exploited to quantify plant phenolics remains to be fully tested. The tea polyphenols related to the 1.66 μm feature in this study are comprised of a single class of condensed tannins (based on catechins or flavan-3-ols). More study is needed to examine the strength of this relationship with other plant phenolics, including other condensed tannins and hydrolysable tannins. Notably, this study did not address the potential indi-

cated by some recent studies in using spectra collected by airborne imaging spectrometers for quantifying and mapping plant phenolic concentrations across a landscape.

Spectra of sagebrush leaves, evergreen needles, and canopies of these plants showed an absorption feature with a center near 1.63 μm. This feature is shifted 30 nm short ward of absorption features in phenolic compounds. Elevated levels of terpene compounds can sometimes be found in these vegetation types. An absorption feature of the terpene camphene was found at 1.639 μm, close to the absorption seen in spectra of sagebrush and conifers. More work is needed to validate that terpenes cause the absorptions seen in the leaf and canopy spectra of these plants.

This study contributes to the body of literature that shows that subtle variation in vegetation spectra in the SWIR can directly indicate biochemical constituents of lesser abundance than the major plant components. Though of lower abundance, these components have important plant functions. Dry leaf spectra should not all be assumed to be the same. The gross changes wrought by structural biochemical constituents, such as lignin and cellulose, and small variations caused by phenolics can both contribute to spectral discrimination of species. The demonstrated links between phenolic absorption features and those evident in plant spectra, and high correlations between the 1.66 μm feature and phenolic concentrations, support past studies showing statistical success in predicting phenolic concentration estimates from reflectance, even at the canopy level. New detailed studies are warranted to advance our knowledge of the spectral influences of plant phenolics of various types (e.g., condensed and hydrolysable tannins) relative to dominant biochemistry (water, chlorophyll, nitrogen, cellulose, and lignin). Especially challenging to our comprehension is the influence of plant phenolics when concentrations are low and less prominent in spectra. Leaf and canopy models represent one potential avenue for advancing that understanding. The development of a greater understanding of vegetation reflectance could be significantly assisted by large public databases of spectra and related chemistry that go beyond basic plant constituents by including phenolics, terpenes, proteins, amino acids, starch, hemicellulose, sugars, and other important plant components.

## Acknowledgments

The authors are grateful for the tea spectra and phenolic data shared by Meng Bian and Teng Fei and the benzene spectrum shared by Roger Clark. The U.S. Geological Survey's Mineral Resources Program provided salary and materials support for R.F. Kokaly. Any use of trade, firm, or product names is for descriptive purposes only and does not imply endorsement by the U.S. Government.

## References

ACCP, 19 October 1994. Accelerated Canopy Chemistry Program Final Report to NASA-EOS-IWG. National Aeronautics and Space Administration, Washington D.C.

Aguero, M.E., Gevens, A., Nicholson, R.L., 2002. Interaction of *Cochliobolus heterostrophus* with phytoalexin inclusions in Sorghum bicolor. Physiol. Mol. Plant Pathol. 61, 267–271.

Ainsworth, E.A., Gillespie, K.M., 2007. Estimation of total phenolic content and other oxidation substrates in plant tissues using Folin-Ciocalteu reagent. Nat. Protoc. 2, 875–877.

Asner, G.P., Martin, R.E., Bin Suhaili, A., 2012. Sources of canopy chemical and spectral diversity in lowland Bornean forest. Ecosystems 15, 504–517, http://dx.doi.org/10.1007/s10021-012-9526-2.

Asner, G.P., Martin, R.E., Knapp, D.E., Tupayachi, R., Anderson, C., Carranza, L., Martinez, P., Houcheime, M., Sinca, F., Weiss, P., 2011. Spectroscopy of canopy chemicals in humid tropical forests. Remote Sens. Environ. 115, 3587–3598 http://dx.doi.org/10.1016/j.rse.2011.08.020

Baldwin, I.T., Schultz, J.C., Ward, D., 1987. Patterns and sources of leaf tannin variation in yellow birch (*Betula allegheniensis*) and sugar maple (*Acer saccharum*). J. Chem. Ecol. 13 (5), 1069–1078.

Barbehenn, R.V., Constabel, C.P., 2011. Tannins in plant–herbivore interactions. Phytochemistry 72, 1551–1565.

Barton, F.E., Himmelsbach, D.S., 1993. Two-dimensional vibrational spectroscopy II: correlation of the absorptions of lignins in the mid- and near-infrared. Appl. Spectrosc. 47, 1920–1925.

Bate-Smith, E.C., 1977. Astringent tannins of *Acer* species. Phytochemistry 16 (9), 1421–1426.

Bate-Smith, E.C., Swain, T., 1962. Comparative Biochemistry. In: Mason, H.S., Florkin, A.M. (Eds.). Springer, Berlin.

Ben-Dor, E., Inbar, Y., Chen, Y., 1997. The reflectance spectra of organic matter in the visible near-infrared and short wave infrared region (400–2500 nm) during a controlled decomposition process. Remote Sens. Environ. 61, 1–15.

Bian, M., Skidmore, A.K., Schlerf, M., Wang, T., Liu, Y., Zeng, R., Fei, T., 2013. Predicting foliar biochemistry of tea (Camellia sinensis) using reflectance spectra measured at powder, leaf and canopy levels. ISPRS J. Photogramm. Remote Sens. 78, 148–156 http://dx.doi.org/10.1016/j.isprsjprs.2013.02.002

Bian, M., Skidmore, A.K., Schlerf, M., Fei, T., Liu, Y., Wang, T., 2010. Reflectance spectroscopy of biochemical components as indicators of tea (*Camellia Sinensis*) quality. Photogramm. Eng. Remote Sens. 76 (12), 1385–1392.

Bolster, K.L., Martin, M.E., Aber, J.D., 1996. Determination of carbon fraction and nitrogen concentration in tree foliage by near infrared reflectance: a comparison of statistical methods. Can. J. Forest Res. 26, 590–600.

Bryant, J.P., Chapin III, F.S., Reichardt, Clausen, P.B., 1987. Response of winter chemical defense in Alaska paper birch and green alder to manipulation of plant carbon/nutrient balance. Oecologia 72 (4), 510–514.

Cameron, D.G., Kauppinen, J.K., Moffat, D.J., Mantsch, H.H., 1982. Precision in condensed phase vibrational spectroscopy. Appl. Spectrosc. 36, 245–250.

Campbell, P.K.E., Rock, B.N., Martin, M.E., Neefus, C.D., Irons, J.R., Middleton, E.M., Albrechtová, J., 2004. Detection of initial damage in Norway spruce canopies using hyperspectral airborne data. Int. J. Remote Sens. 25 (24), 5557–5584.

Choquette, S.J., Travis, J.C., Duewer, D.L., 1998. SRM 2035—A rare earth oxide glass for the wavelength calibration of near infrared dispersive and Fourier transform spectrometers. In Conference on optical diagnostic methods for inorganic transmission materials, 1998, international society for optical engineering In: Proceedings: Bellingham, Wash., 3425, pp. 94–102.

Chou, C.H., Muller, C.H., 1972. Allelopathic mechanisms of *Arctostaphylos glandulosa* var. *zacaensis*. Am. Midl. Nat. 88 (2), 324–347.

Clark, R.N., Curchin, J.M., Barnes, J.W., Jaumann, R., Soderblom, L., Cruikshank, D.P., Brown, R.H., Rodriguez, S., Lunine, J., Stephan, K., Hoefen, T.M., et al., 2010. Detection and mapping of hydrocarbon deposits on Titan. J. Geophys. Res. 115, E10005 http://dx.doi.org/10.1029/2009JE003369

Clark, R.N., Swayze, G.A., Livo, K.E., Kokaly, R.F., Sutley, S.J., Dalton, J.B., McDougal, R.R., Gent, C.A., 2003. Imaging spectroscopy: earth and planetary remote sensing with the USGS tetracorder and expert systems. J. Geophys. Res. 108 (E12), 5131–5146.

Clark, R.N., Swayze, G.A., Livo, K.E., Kokaly, R.F., King, T.V.V., Dalton, J.B., Vance, S., Rockwell, B.R., Hoefen, T., McDougal, R.R., 2002. Surface reflectance calibration of terrestrial imaging spectroscopy data: A tutorial using AVIRIS. Proceedings of the 10th airborne earth science workshop, JPL Publication, 1–2 http://speclab.cr.usgs.gov/PAPERS.calibration.tutorial/

Clark, R.N., 1999. Spectroscopy of rocks and minerals and principles of spectroscopy. In: Rencz, A.N. (Ed.), Remote Sensing for the Earth Sciences: Manual of Remote Sensing, 3, 3rd ed. Wiley, New York, pp. 3–58.

Clark, R.N., 1993. SPECtrum processing routines user's manual version 3 (program SPECPR): U.S Geological Survey Open-File Report 93–595, 210 p. http://speclab.cr.usgs.gov

Clark, R.N., Gallagher, A.J., Swayze, G.A., 1990. Material absorption band depth mapping of imaging spectrometer data using a complete band shape least-squares fit with library reference spectra. In: Green, R.O. (Ed.), Proceedings of the Second Airborne Visible/infrared Imaging Spectrometer (AVIRIS) Workshop, 90-54. JPL Publication, pp. 176–186.

Clark, R.N., Roush, T.L., 1984. Reflectance spectroscopy: quantitative analysis techniques for remote sensing applications. J. Geophys. Res. 89, 6329–6340.

Cloutis, E.A., 1989. Spectral reflectance properties of hydrocarbons: remote-sensing implications. Science 245, 165–168.

Crawford, R.L., 1981. Lignin biodegradation and transformation. Wiley Interscience, New York.

Curran, P.J., 1989. Remote sensing of foliar chemistry. Remote Sens. Environ. 30 (3), 271–278.

de Candolle, A.P., Theorie elementaire de la botanique ou Exposition des principes de la classification naturelle et de l'art de decrire et d'etudier les vegetaux Chez Deterville, libraire, rue Hautefeuille, n. o8, Paris 1813.

Déyeux, C., 1793. Sur la Noix de Galle. Ann. Chim. 17, 3–66.

Elvidge, C.D., 1990. Visible and near infrared reflectance characteristics of dry plant materials. Int. J. Remote Sens. 11 (10), 1775–1795.

Feeny, P., 1970. Seasonal changes in oak leaf tannins and nutrients as a cause of spring feeding by winter moth caterpillars. Ecology 51 (4), 565–581.

Ferwerda, J.G., Skidmore, A.K., Stein, A., 2006. A bootstrap procedure to select hyperspectral wavebands related to tannin content. Int. J. Remote Sens. 27 (7), 1413–1424.

Foley, W.J., McIlwee, A., Lawler, I., Aragones, L., Woolnough, A.P., Berding, N., 1998. Ecological applications of near infrared reflectance spectroscopy: a tool for rapid, cost-effective prediction of the composition of plant and animal tissues and aspects of animal performance. Oecologia 116 (3), 293–305.

Flinn, P.C., Edwards, N.J., Oldham, C.M., McNeil, D.M., 1996. Near infrared analysis of the fodder shrub tagaste (*Chamaecytisus proliferus*) for nutritive value and anti-nutritive factors. In: Davies, A.M.C., Williams, P. (Eds.), Near Infrared Spectroscopy: The Future Waves. NIR, Chichester, pp. 576–580.
Folin, O., Ciocalteu, V., 1927. On tyrosine and tryptophane determinations in proteins. J. Biol. Chem. 73, 627–650.
Gao, B.-C., Goetz, A.F.H., 1994. Extraction of dry leaf spectral features from reflectance spectra of green vegetation. Remote Sens. Environ. 47 (3), 369–374.
Gao, B.-C., Goetz, A.F.H., 1995. Retrieval of equivalent water thickness and information related to biochemical components of vegetation canopies from AVIRIS data. Remote Sens. Environ. 52 (3), 155–162.
Girma, A., Skidmore, A.K., de Bie, C.A.J.M., Bongers, F., Schlerf, M., 2013. Photosynthetic bark: use of chlorophyll absorption continuum index to estimate *Boswellia papyrifera* bark chlorophyll content. Int. J. Appl. Earth Obs. Geoinf. 23, 71–80.
Haslam, E., 2007. Vegetable tannins–lessons of a phytochemical lifetime. Phytochemistry 68, 2713–2721.
Haslam, E., 1989. Plant polyphenols: vegetable tannins revisited. Cambridge University Press, Cambridge UK.
Haslam, E., 1965. Galloyl esters in the *Aceraceae*. Phytochemistry 4 (3), 495–498.
Hatfield, R., Vermerris, W., 2001. Lignin formation in plants. The dilemma of linkage specificity. Plant Physiol. 126 (4), 1351–1357.
Huang, D., Ou, B., Prior, R.L., 2005. The chemistry behind antioxidant capacity assays. J. Agric. Food Chem. 53, 1841–1856.
Jacquemoud, S., Baret, F., 1990. PROSPECT: a model of leaf optical properties spectra. Remote Sens. Environ. 34, 75–91.
Jacquemoud, S., Verhoef, W., Baret, F., Bacour, C., Zarco-Tejada, P.J., Asner, G.P., Francois, C., Ustin, S.L., 2009. PROSPECT+ SAIL models: a review of use for vegetation characterization. Remote Sens. Environ. 113, S56–S66.
Johnson, L.F., Billow, C.R., 1996. Spectrometric estimation of total nitrogen concentration in Douglas-fir foliage. Int. J. Remote Sens. 17, 489–500.
Kelsey, R.G., Wright, W.E., Forrest, S., Winward, A., Britton, C., 1983. The concentration and composition of big sagebrush essential oils from Oregon. Biochem. Syst. Ecol. 11 (4), 353–360.
Kokaly, R.F., Couvillion, B.R., Holloway, J.M., Roberts, D.A., Ustin, S.L., Peterson, S.H., Khanna, S., Piazza, S.C., 2013. Spectroscopic remote sensing of the distribution and persistence of oil from the Deepwater Horizon spill in Barataria Bay marshes. Remote Sens. Environ. 129, 210–230 http://dx.doi.org/10.1016/j.rse.2012.10.028
Kokaly, R.F., 2011. PRISM: processing routines in IDL for spectroscopic measurements (installation manual and user's guide, version 1. 0). U.S. Geological Survey Open-File Report, 1155 http://pubs.usgs.gov/of/2011/1155/
Kokaly, R.F., Asner, G.P., Ollinger, S.V., Martin, M.E., Wessman, C.A., 2009. Characterizing canopy biochemistry from imaging spectroscopy and its application to ecosystem studies. Remote Sens. Environ. 113, S78–S91 http://dx.doi.org/10.1016/j.rse.2008.10.018
Kokaly, R.F., Rockwell, B.W., Haire, S.L., King, T.V.V., 2007. Characterization of postfire surface cover, soils, and burn severity at the Cerro Grande Fire, New Mexico, using hyperspectral and multispectral remote sensing. Remote Sens. Environ. 106, 305–325 http://dx.doi.org/10.1016/j.rse.2006.08.006
Kokaly, R.F., Despain, D.G., Clark, R.N., Livo, K.E., 2003. Mapping vegetation in Yellowstone National Park using spectral feature analysis of AVIRIS data. Remote Sens. Environ. 84, 437–456 http://dx.doi.org/10.1016/S0034-425(02)133-5
Kokaly, R.F., 2001. Investigating a physical basis for spectroscopic estimates of leaf nitrogen concentration. Remote Sens. Environ. 75, 153–161 http://dx.doi.org/10.1016/S0034-4257(00)163-2
Kokaly, R.F., Clark, R.N., 1999. Spectroscopic determination of leaf biochemistry using band-depth analysis of absorption features and stepwise multiple linear regression. Remote Sens. Environ. 67, 267–287 http://dx.doi.org/10.1016/S0034-4257(98)84-4
Lopes-Lutz, D., Alviano, D.S., Alviano, C.S., Kolodziejczyk, P.P., 2008. Screening of chemical composition, antimicrobial and antioxidant activities of Artemisia essential oils. Phytochemistry 8, 1732–1738 http://dx.doi.org/10.1016/j.phytochem.2008.02.014
Malenovský, Z., Homolová, L., Zurita-Milla, R., Lukeš, P., Kaplan, V., Hanuš, J., Gastellu-Etchegorry, J., Schaepman, M.E., 2013. Retrieval of spruce leaf chlorophyll content from airborne image data using continuum removal and radiative transfer. Remote Sens. Environ. 131, 85–102.
Martin, M.E., Aber, J.D., 1997. High spectral resolution remote sensing of forest canopy lignin, nitrogen, and ecosystem processes. Ecol. Appl. 7, 431–443.
Meggio, F., Zarco-Tejada, P.J., Núñez, L.C., Sepulcre-Cantó, G., González, M.R., Martín, P., 2010. Grape quality assessment in vineyards affected by iron deficiency chlorosis using narrow-band physiological remote sensing indices. Remote Sens. Environ. 114 (9), 1968–1986 http://dx.doi.org/10.1016/j.rse.2010.04.004
Mitchell, J.J., Glenn, N.F., Sankey, T.T., Derryberry, D.R., Anderson, M.O., Hruska, R.C., 2012. Spectroscopic detection of nitrogen concentrations in sagebrush. Remote Sens. Lett. 3:4, 285–294 http://dx.doi.org/10.1080/01431161.2011.580017
Mueller-Harvey, I., 2001. Analysis of hydrolysable tannins. Anim. Feed Sci. Technol. 91, 3–20.
Muller, C.H., Hanawalt, R.B., McPherson, J.K., 1968. Allelopathic control of herb growth in the fire cycle of California chaparral. Bull. Torrey Bot. Club 95 (3), 225–231.
Mustard, J.F., Sunshine, J.M., 1999. Spectral analysis for Earth science investigation. In: Rencz, A.N. (Ed.), Remote sensing for the earth sciences: manual of remote sensing, 3, 3rd ed. Wiley, New York, pp. 251–306.
Newman, S.D., Soulia, M.E., Aber, J.D., Dewey, B., Ricca, A., 1994. Analyses of forest foliage I: laboratory procedures for proximate carbon fractionation and nitrogen determination. J. Near Infrared Spectrosc. 2, 5–14.
Norris, K.H., Barnes, R.F., Moore, J.E., Shenk, J.S., 1976. Predicting forage quality by infrared reflectance spectroscopy. J. Animal Sci. 43, 889–897.
Paaver, U., Matto, V., Raal, A., 2010. Total tannin content in distinct *Quercus robur* L. galls. J. Med. Plants Res. 4 (8), 702–705.
Pureswaran, D.S., Gries, R., Borden, J.H., 2004. Quantitative variation in monoterpenes in four species of conifers. Biochem. Syst. Ecol. 32, 1109–1136.
Ramoelo, A., Skidmore, A.K., Schlerf, M., Mathieu, R., Heitkönig, I.M.A., 2011. Water-removed spectra increase the retrieval accuracy when estimating savanna grass nitrogen and phosphorus concentrations. ISPRS J. Photogramm. Remote Sens. 66, 408–417.
Rice-Evans, C.A., Miller, N.J., Paganga, G., 1996. Structure-antioxidant activity relationships of flavonoids and phenolic acids. Free Radical Biol. Med. 20 (7), 933–956.
Roberts, D.A., Ustin, S.L., Ogunjemiyo, S., Greenberg, J., Dobrowski, S.Z., Chen, J., Hinckley, T.M., 2004. Spectral and structural measures of northwest forest vegetation at leaf to landscape scales. Ecosystems 7, 545–562 http://dx.doi.org/10.1007/s10021-004-0144-5
Salminen, J.P., Karonen, M., 2011. Chemical ecology of tannins and other phenolics: we need a change in approach. Funct. Ecol. 25, 325–338.
Sanches, I., Souza Filho, C.R., Kokaly, R.F., 2014. Spectroscopic remote sensing of plant stress at leaf and canopy levels using the chlorophyll 680 nm absorption feature with continuum removal. ISPRS J. Photogramm. Remote Sens. 97, 111–122 http://dx.doi.org/10.1016/j.isprsjprs.2014.08.015
Savitzky, A., Golay, M.J.E., 1964. Smoothing and differentiation of data by simplified least squares procedures. Anal. Chem. 36, 1627–1639.
Schaepman, M.E., Ustin, S.L., Plaza, A.J., Painter, T.H., Verrelst, J., Liang, S., 2009. Earth system science related imaging spectroscopy—an assessment. Remote Sens. Environ. 113, S123–S137.
Schaepman-Strub, G., Schaepman, M.E., Painter, T.H., Dangel, S., Martonchik, J.V., 2006. Reflectance quantities in optical remote sensing—definitions and case studies. Remote Sens. Environ. 103 (1), 27–42.
Schanda, E., 1986. Physical Fundamentals of Remote Sensing. Springer-Verlag, New York.
Schultz, J.C., Baldwin, I.T., 1982. Oak leaf quality declines in response to defoliation by gypsy moth larvae. Science 217 (4555), 149–151.
Seguin, A., 1796. Sur les nouveaux moyens de tanner les cuirs. Ann. Chim. 20, 15–77.
Shure, D.J., Mooreside, P.D., Ogle, S.M., 1998. Rainfall effects on plant-herbivore processes in an upland oak forest. Ecology 79 (2), 604–617.
Singleton, V.L., Rossi, J.A., 1965. Colorimetry of total phenolics with phosphomolybdic-phosphotungstic acid reagents. Am. J. Enol. Vitic. 16 (3), 144–158.
Singleton, V.L., Orthofer, R., Lamuela-Raventos, R.M., 1999. Analysis of total phenols and other oxidation substrates and antioxidants by means of Folin-Ciocalteu reagent. Methods Enzymol. 299, 152–178.
Skidmore, A.K., Ferwerda, J.G., Mutanga, O., Van Wieren, S.E., Peel, M., Grant, R.C., Prins, H.H.T., Balcik, F.B., Venus, V., 2010. Forage quality of savannas—simultaneously mapping foliar protein and polyphenols for trees and grass using hyperspectral imagery. Remote Sens. Environ. 114, 64–72.
Soukupová, J., Rock, B.N., Albrechtová, J., 2002. Spectral characteristics of lignin and soluble phenolics in the near infrared–a comparative study. Int. J. Remote Sens. 23 (15), 3039–3055.
Soukupová, J., Rock, B.N., Albrechtová, J., 2001. Comparative study of two spruce species in a polluted mountainous region. New Phytol. 150, 133–145.
Stevanato, R., Fabris, S., Momo, F., 2004. Enzymatic method for the determination of total phenolic content in tea and wine. J. Agric. Food Chem. 52, 6287–6293.
Swain, T., 1965. The tannins. In: Bonner, J., Varner, J.E. (Eds.), Plant Biochemistry. Academic Press, New York, pp. 552–580.
Swayze, G.A., Kokaly, R.F., Higgins, C.T., Clinkenbeard, J.P., Clark, R.N., Lowers, H.A., Sutley, S.J., 2009. Mapping potentially asbestos-bearing rocks using imaging spectroscopy. Geology 37, 763–766 http://dx.doi.org/10.1130/G30114A.1
Tolbert, A., Akinosho, H., Khunsupat, R., Naskar, A.K., Ragauskas, A.J., 2014. Characterization and analysis of the molecular weight of lignin for biorefining studies. Biofuels, Bioprod. Biorefin. 8, 836–856 http://dx.doi.org/10.1002/bbb.1500
Ustin, S.L., Gitelson, A.A., Jacquemoud, S., Schaepman, M., Asner, G.P., Gamon, J.A., Zarco-Tejada, P., 2009. Retrieval of foliar information about plant pigment systems from high resolution spectroscopy. Remote Sens. Environ. 113, S67–S77.
van Etten, H.D., Mansfield, J.W., Bailey, J.A., Farmer, E., 1994. Two classes of plant antibiotics: phytoalexins versus phytoanticipins. Plant Cell 6, 1191–1192.
van Ruitenbeek, F.J.A., Bakker, W.H., van der Werff, H.M.A., Zegers, T.E., Oosthoek, J.H.P., Omer, Z.A., Marsh, S.H., van der Meer, F.D., 2014. Mapping the wavelength position of deepest absorption features to explore mineral diversity in hyperspectral images. Planet. Space Sci. 101, 108–117 http://dx.doi.org/10.1016/j.pss.2014.06.009
Vermerris, W., Nicholson, R., 2006. Phenolic Compound Biochemistry. Springer, Netherlands.
Wheeler, O.H., 1959. Near infrared spectra of organic compounds. Chem. Rev. 59 (4), 629–666.

Wilson, N.D., Watt, R.A., Moffat, A.C., 2001. A near-infrared method for the assay of cineole in eucalyptus oil as an alternative to the official BP method. J. Pharm. Pharmacol. 53, 95–102.
Wilt, F.M., Miller, G.C., 1992. Seasonal variation of coumarin and flavonoid concentrations in persistent leaves of Wyoming big sagebrush (*Artemisia tridentata* ssp. *wyomingensis*: asteraceae). Biochem. Syst. Ecol. 20 (1), 53–67.
Windham, W.R., Fales, S.L., Hoveland, C.S., 1988. Analysis for tannin concentration in Sericea lespedeza by near infrared reflectance spectroscopy. Crop Sci. 28, 705–708.
Zucker, W.V., 1983. Tannins: does structure determine function? an ecological perspective. Am. Nat. 121 (3), 335–365.